

# Variational optimization approach for reconstruction of dielectric permittivity and conductivity functions using partial boundary measurements

E. Lindström \*      L. Beilina †

February 10, 2026

## Abstract

We present a variational optimization approach for the solution of a coefficient inverse problem of simultaneous reconstruction of the dielectric permittivity and conductivity functions in time-dependent Maxwell's system using limited boundary observations of the electric field.

The variational optimization approach is based on constructing a weak form of a Lagrangian which allows to use finite element based reconstruction algorithms. The optimality conditions for the Lagrangian and stability estimate for the adjoint problem are derived, as well as Frechét differentiability of it and of the regularized Tikhonov functional are also presented. Two- and three-dimensional numerical studies confirm our theoretical investigations.

*Keywords:* Maxwell's system, coefficient inverse problem, Tikhonov functional, Lagrangian approach, stability analysis, conjugate gradient algorithm

*MSC 2010:* 65M06, 65M60, 65M22, 65M32

## 1 Introduction

In this work we present analysis of variational optimization approach for reconstruction of spatially distributed dielectric permittivity and conductivity functions using partial time-dependent measurements of the scattered electric field at the part of the boundary of investigated domain. This problem is a typical coefficient inverse problem (CIP) where both coefficients of the time-dependent Maxwell's equations, dielectric permittivity and conductivity functions, should be reconstructed from boundary measurements. These coefficients describe a spatially distributed property of the medium

---

\*Eric Lindström, Email: erilinds@chalmers.se

†Larisa Beilina, Email: larisa.beilina@chalmers.se

Department of Mathematical Sciences, Chalmers University of Technology and University of Gothenburg, SE-412 96 Gothenburg Sweden

of interest. Hence, quantitative and qualitative reconstruction of these coefficients leads to an image of the interior of the medium and to quantitative estimation of these parameters.

It is well known that CIPs are ill-posed problems [4, 19, 26, 39, 40]. In previous studies [11, 13, 37, 38], a novel non-local, approximately globally convergent method for reconstructing the dielectric permittivity function was developed and validated through numerical experiments. In above cited works the scalar wave equation was taken as an approximate mathematical model for the Maxwell's equations. The two-stage global adaptive optimization method was introduced in [11] for reconstructing the dielectric permittivity function in non-conductive media. The two-stage numerical procedure of [11] was verified in several works [13, 37, 38] on experimental data collected by the microwave scattering facility.

The experimental and numerical tests of above cited works show that developed methods provide accurate imaging of all three components of interest in imaging of targets: shapes, locations and refractive indices of non-conductive media. In [29], see also references therein, authors show reconstruction of complex dielectric permittivity function using convexification method and frequency-dependent data. Potential applications of all above cited works are in the detection and characterization of improvised explosive devices (IEDs).

In contrast to the previously cited works, this study presents a theoretical and numerical analysis of a variational optimization approach for solving the coefficient inverse problem for a stabilized Maxwell system in conductive media, based on the construction of a Lagrangian associated with a regularized Tikhonov functional. The optimality conditions for the Lagrangian, as well as stability estimates for the adjoint problem, are rigorously derived. In addition, the Fréchet differentiability of both the adjoint problem and the regularized Tikhonov functional is established.

The numerical examples presented in this work demonstrate that both two- and three-dimensional conjugate gradient (CGA) and adaptive conjugate gradient (ACGA) algorithms can efficiently and accurately reconstruct the dielectric permittivity and conductivity functions using backscattered electric field data. While the two-dimensional examples are primarily of theoretical interest, the three-dimensional numerical results focus on applications in microwave medical imaging, specifically the detection of malignant melanoma, MM.

We note that one of the most important application of algorithms of this paper is microwave imaging including microwave medical imaging [1, 2, 7] and imaging of improvised explosive devices (IEDs) [11] where qualitative and quantitative determination of both, the dielectric permittivity and electric conductivity functions from boundary measurements, is needed. Potential application of theory and algorithms developed in this work are in cancer detection using microwaves. Previous studies [7, 27] have highlighted variations in the relative dielectric permittivity and conductivity contrasts between malignant and normal tissues, demonstrating that malignant tumors exhibit higher relative permittivity values compared to normal tissues at frequencies below 10 GHz. Several engineering works have tackled this issue - see some of them in [1, 2, 7] and references therein. See also recent studies [5, 6, 9] where authors have reported first results for the detection of breast cancer and malignant melanoma (MM) using variational optimization approach analyzed in this work. It is worth noting that mi-

crowave medical imaging, when based solely on boundary measurements of backscattered electric waves at frequencies around 1 GHz, represents a non-invasive imaging technique. Thus, it is very attractive addition to the existing imaging technologies like X-ray mammography [20, 41], ultrasound [23, 24] and MRI imaging [25]. We have performed numerical tests on the reconstruction of MM using two of the real-life MM models developed in the recent work [10] with realistic weighted dielectric properties of MM at 6 GHz taken from [6, 7].

The main contributions of our paper can be summarized as follows:

- Derivation of the weak formulation of the Lagrangian and optimality conditions of the Lagrangian in the weak form.
- Derivation of stability estimate for the adjoint problem.
- Proof the Fréchet differentiability of the regularized Tikhonov's functional in the weak form.
- Proof of the existence of the minimizers for the non-regularized and regularized Tikhonov's functionals.
- Two- and three-dimensional numerical tests which validate developed variational optimization technique via CGA and ACGA algorithms.

An outline of the work is as follows: in section 2 we present the mathematical model and formulate CIP. Section 3 introduces Tikhonov's functional and the Lagrangian in the weak form and shows proofs for optimality conditions of the Lagrangian in a weak form. Section 4 formulates energy estimate for the forward problem and establishes stability result for the adjoint problem. Section 5 presents mathematical analysis of the optimization problem and Section 6 presents proof for the existence of the minimizer. Section 7 presents CGA and ACGA algorithms and Section 8 shows two- and three-dimensional numerical examples of reconstruction of both dielectric permittivity and conductivity functions. Finally, section 9 discusses obtained results and future research.

## 2 The mathematical model

Let us consider the Cauchy problem for Maxwell's equations in  $\mathbb{R}^d$ ,  $d = 2, 3$ , in inhomogeneous conductive media:

$$\begin{cases} \partial_t B = -\nabla \times E & \text{for } (x, t) \in \mathbb{R}^d \times (0, \infty), & (2.1a) \\ \partial_t D = \nabla \times H - \sigma E - J & \text{for } (x, t) \in \mathbb{R}^d \times (0, \infty), & (2.1b) \\ \nabla \cdot D = 0 & \text{for } (x, t) \in \mathbb{R}^d \times (0, \infty), & (2.1c) \\ E(x, 0) = f_0, \partial_t E(x, 0) = f_1 & \text{for } x \in \mathbb{R}^d, & (2.1d) \end{cases}$$

where  $B$ ,  $E$ ,  $D$ ,  $H$  and  $J$  are time-dependent vector fields in  $\mathbb{R}^d$  representing the magnetic flux density, the electric field, the electric flux density, the magnetic field and the

electric current density respectively, and  $\sigma$  is a spatial function representing the conductivity. We also have vector valued  $f_0$  and  $f_1$  which are arbitrary initial conditions.

This article will handle linear and isotropic materials, which implies

$$D = \varepsilon E \text{ and } B = \mu H, \quad (2.2)$$

where the electric permittivity  $\varepsilon(x) = \varepsilon_0 \varepsilon_r(x)$  and the magnetic permeability  $\mu(x) = \mu_0 \mu_r(x)$  are spatial scalar functions. Now we can rewrite (2.1a) in terms of  $E$ ,  $H$  and  $J$  as

$$\begin{cases} \mu \partial_t H = -\nabla \times E & \text{for } (x, t) \in \mathbb{R}^d \times (0, \infty), & (2.3a) \\ \varepsilon \partial_t E = \nabla \times H - \sigma E - J & \text{for } (x, t) \in \mathbb{R}^d \times (0, \infty), & (2.3b) \\ \nabla \cdot (\varepsilon E) = 0 & \text{for } (x, t) \in \mathbb{R}^d \times (0, \infty), & (2.3c) \\ E(x, 0) = f_0, \partial_t E(x, 0) = f_1 & \text{for } x \in \mathbb{R}^d, & (2.3d) \end{cases}$$

From here we will take the time-derivative of (2.3b) to be able to merge it with (2.3a). This gives us the equation

$$\varepsilon \partial_{tt} E = -\nabla \times \left( \frac{1}{\mu} \nabla \times E \right) - \sigma \partial_t E - \partial_t J. \quad (2.4)$$

Moving all terms dependent on  $E$  of the (2.4) to the left side after merging the first two equations we end up with the system

$$\begin{cases} \varepsilon \partial_{tt} E + \sigma \partial_t E + \nabla \times \left( \frac{1}{\mu} \nabla \times E \right) = -\partial_t J & \text{for } (x, t) \in \mathbb{R}^d \times (0, \infty), & (2.5a) \\ \nabla \cdot (\varepsilon E) = 0 & \text{for } (x, t) \in \mathbb{R}^d \times (0, \infty), & (2.5b) \\ E(x, 0) = f_0, \partial_t E(x, 0) = f_1 & \text{for } x \in \mathbb{R}^d, & (2.5c) \end{cases}$$

In this article we will consider solution of CIP in the non-magnetic object, or assume that  $\mu_r \equiv 1$ , which is roughly the case for human tissues. We will also note the theoretical connection between  $\varepsilon_0$ ,  $\mu_0$  and the speed of light  $c$ , namely  $c = (\varepsilon_0 \mu_0)^{-1/2}$ . This allows us to rewrite our system once again into

$$\begin{cases} \frac{\varepsilon_r}{c^2} \partial_{tt} E + \mu_0 \sigma \partial_t E + \nabla \times \nabla \times E = -\mu_0 \partial_t J & \text{for } (x, t) \in \mathbb{R}^d \times (0, \infty), & (2.6a) \\ \nabla \cdot (\varepsilon_r E) = 0 & \text{for } (x, t) \in \mathbb{R}^d \times (0, \infty), & (2.6b) \\ E(x, 0) = f_0, \partial_t E(x, 0) = f_1 & \text{for } x \in \mathbb{R}, & (2.6c) \end{cases}$$

The issue with (2.6a–d) is that  $c^{-2}$  and  $\mu_0$  are very small constants, the former even smaller than expected accuracy from double precision float points. To contend with this we will substitute  $t := ct$ , such that we can instead inspect

$$\begin{cases} \varepsilon_r \partial_{tt} E + c \mu_0 \sigma \partial_t E + \nabla \times \nabla \times E = -c \mu_0 \partial_t J & \text{for } (x, t) \in \mathbb{R}^d \times (0, \infty), & (2.7a) \\ \nabla \cdot (\varepsilon_r E) = 0 & \text{for } (x, t) \in \mathbb{R}^d \times (0, \infty), & (2.7b) \\ E(x, 0) = f_0, \partial_t E(x, 0) = f_1 & \text{for } x \in \mathbb{R}, & (2.7c) \end{cases}$$

*Remark:* For the convenience, since we are interested in reconstruction of  $\varepsilon_r$  and  $\sigma$ , we will simplify the notation and omit the subscript  $r$  from  $\varepsilon_r$  and include the constants in  $\sigma$ . Thus  $\varepsilon := \varepsilon_r$  (which should not be confused with the absolute electric permittivity) and  $\sigma := c\mu_0\sigma$  from now. Similarly, we will let  $\partial_t J := c\mu_0\partial_t J$ .

For this application we will restrict ourselves to a bounded, convex domain  $\Omega \subset \mathbb{R}^d$  with the smooth boundary  $\Gamma$ . We will also denote the corresponding space-time domain as  $\Omega_T := \Omega \times (0, T)$  with the space-time boundary  $\Gamma_T := \Gamma \times (0, T)$ , where  $T > 0$  is the final time. Further, we will consider the stabilized model problem by introducing the Coulomb gauge-type term (2.7b) in (2.7a) (see details in [3, 32]) and thus consider

$$\begin{cases} \varepsilon \partial_{tt} E + \sigma \partial_t E - \Delta E - \nabla \nabla \cdot (\varepsilon - 1) E = -\partial_t J & \text{for } (x, t) \in \Omega_T, & (2.8a) \\ E(x, 0) = f_0, \partial_t E(x, 0) = f_1 & \text{for } x \in \Omega, & (2.8b) \\ \partial_n E = 0 & \text{for } (x, t) \in \Gamma_T. & (2.8c) \end{cases}$$

In recent work [12] it was shown that under sufficient conditions on  $\varepsilon$  and  $\sigma$  the system above approximates the original Maxwell's equations well. We denote the task of finding the field  $E$  as the forward problem.

Before we state the inverse problem we will introduce the domain decomposition (see [5]). We will assume  $\bar{\Omega} = \Omega_{\text{FDM}} \cup \Omega_{\text{FEM}}$  and  $\Omega_{\text{FEM}} \subset \Omega$  as well as  $\partial\Omega_{\text{FEM}} \subset \Omega_{\text{FDM}}$ . For the sake of convenience we will also introduce  $\Omega_{\text{IN}} := \Omega \setminus \Omega_{\text{FDM}}$ . With this setup we will add some realistic assumptions on  $\sigma$  and  $\varepsilon$  in terms of two parameters sets

$$\begin{aligned} \varepsilon \in C_\varepsilon &:= \{\varepsilon \in C^2(\bar{\Omega}) : \varepsilon(x) = 1 \quad \forall x \in \Omega_{\text{FDM}}, 1 \leq \varepsilon(x) \leq d_1 \quad \forall x \in \Omega_{\text{IN}}\}, \\ \sigma \in C_\sigma &:= \{\sigma \in C^2(\bar{\Omega}) : \sigma(x) = 1 \quad \forall x \in \Omega_{\text{FDM}}, 1 \leq \sigma(x) \leq d_2 \quad \forall x \in \Omega_{\text{IN}}\}, \end{aligned} \quad (2.9)$$

where  $d_1 \geq 1$  and  $d_2 \geq 0$  are known real constants. We can now state the inverse problem.

**Inverse problem (IP):** Assume that the functions  $\varepsilon \in C_\varepsilon$  and  $\sigma \in C_\sigma$ . For a given observation function  $\tilde{E}_{\text{obs}} \in [L_2(\Gamma_T)]^3$  of the electric field determine  $\varepsilon(x)$  and  $\sigma(x)$  for  $x \in \Omega_{\text{IN}}$  such that

$$E(x, t) = \tilde{E}_{\text{obs}} \quad \forall (x, t) \in \Gamma_T. \quad (2.10)$$

Here,  $E$  is the electric field which satisfy to the system (2.8a–c) and  $\tilde{E}_{\text{obs}}$  is some known boundary measurements.

*Remark:* Note that  $\tilde{E}_{\text{obs}}$  may only be defined on parts of  $\Gamma_T$ , which would correspond to missing data in applications. Usually, this function contains the noise level  $\delta$  which involves ill-posedness of the solution of our IP. Let  $E_{\text{obs}}^*$  denote noiseless exact observations at  $\Gamma_T$  and

$$B_\delta[E_{\text{obs}}^*] = \{E : \|E - E_{\text{obs}}^*\| \leq \delta\}. \quad (2.11)$$

We assume that data  $\tilde{E}_{\text{obs}} \in B_\delta[E_{\text{obs}}^*]$ . In the next section we present the numerical method for solution of ill-posed inverse problem.

### 3 Tikhonov's functional and Lagrangian

Before we move on to defining the corresponding Tikhonov functional and Lagrangian for our problem we will introduce some simplifying notation. We will let the  $L^2$  product of two functions  $f, g : \mathbb{R}^d \rightarrow \mathbb{R}^d$  over some domain  $X$  be denoted by

$$(f, g)_X := \int_X fg \, dX,$$

and the induced norm by  $\|\cdot\|_X$ . If the  $L^2$  in question happens to be a surface integral, we empathize this with brackets,  $\langle f, g \rangle_X$ . Since  $X = \Omega$  and  $X = \Gamma$  will occur frequently we will omit this subscript in those cases. If  $X$  is a set in both space and time we emphasize the  $L^2$  product with double parentheses,  $((f, g))_X$  (or double brackets for surface integrals,  $\langle\langle f, g \rangle\rangle_X$ ), and again in the case where  $X = \Omega_T$  or  $X = \Gamma_T$  we omit the subscript, again for the sake of brevity. Finally, we will let weighted products and norms with a scalar function  $\phi \geq 0$ ,  $\phi \neq 0$  be flagged with a subscript as well, e.g.  $(f, g)_{\phi, X} := (\phi f, g)_X$  and  $\|\cdot\|_{\phi, X}$ .

Now we will move on to define the regularized Tikhonov functional as

$$F(\varepsilon, \sigma) := F(E(\varepsilon, \sigma), \varepsilon, \sigma) = \frac{1}{2} \|E - \tilde{E}_{\text{obs}}\|_{\Gamma_T}^2 + \frac{\gamma_\varepsilon}{2} \|\varepsilon - \varepsilon^0\|^2 + \frac{\gamma_\sigma}{2} \|\sigma - \sigma^0\|^2, \quad (3.1)$$

where  $\gamma_\varepsilon, \gamma_\sigma$  are regularization parameters,  $\delta_{\text{obs}}$  is a  $\delta$ -function with support in some observation points  $x_{\text{obs}}$ , and  $\varepsilon^0, \sigma^0$  are initial guesses for  $\varepsilon$  and  $\sigma$ , respectively. By minimizing the Tikhonov functional we have essentially turned the coefficient inverse problem into an optimization problem.

However, since  $E$  is an implicit function of both  $\varepsilon$  and  $\sigma$ , it is quite difficult to minimize the Tikhonov functional using gradient methods. Therefore we introduce the corresponding Lagrangian, but before we do so we will define some relevant function spaces for  $E$  and  $\lambda$ . Let

$$\begin{aligned} H_E^1 &:= \{E \in [H^1(\Omega_T)]^d : E(x, 0) = f_0(x), \partial_t E(x, 0) = f_1(x) \quad \forall x \in \Omega\}, \\ H_\lambda^1 &:= \{\lambda \in [H^1(\Omega_T)]^d : \lambda(x, T) = 0, \partial_t \lambda(x, T) = 0 \quad \forall x \in \Omega\}, \\ U &:= H_E^1 \times H_\lambda^1 \times C_\varepsilon \times C_\sigma, \end{aligned} \quad (3.2)$$

Next, we will define the Lagrangian, which in strong form looks like

$$L(E, \lambda, \varepsilon, \sigma) = F(E, \varepsilon, \sigma) + ((\varepsilon \partial_{tt} E + \sigma \partial_t E - \Delta E - \nabla \nabla \cdot (\varepsilon - 1)E + \partial_t J, \lambda)). \quad (3.3)$$

However, to assume lower regularity on our solution we will commonly use the weak formulation of  $L(u)$  which we present in the following Lemma.

**Lemma 3.1.** *The weak form of the Lagrangian  $L(u)$  given in (3.3) is*

$$\begin{aligned} L(u) &:= F(E, \varepsilon, \sigma) - (f_1, \lambda(x, 0))_\varepsilon - ((\partial_t E, \partial_t \lambda))_\varepsilon - (f_0, \lambda(x, 0))_\sigma \\ &\quad - ((E, \partial_t \lambda))_\sigma + ((\nabla E, \nabla \lambda)) + ((\nabla \cdot (\varepsilon - 1)E, \nabla \cdot \lambda)) + ((\partial_t J, \lambda)) \end{aligned} \quad (3.4)$$

for  $u := (E, \lambda, \varepsilon, \sigma) \in U$ .

*Proof.* We can prove that the weak form of the Lagrangian simply consists of the Tikhonov functional plus the weak formulation of the forward problem obtained via integration by parts of (3.3). If we assume  $H^2$  regularity on  $E$  and use conditions (2.9) for functions  $\varepsilon, \sigma$  together with  $\lambda(\cdot, T) = \partial_t \lambda(\cdot, T) = 0$ , this is shown as follows:

$$\begin{aligned}
L(E, \lambda, \varepsilon, \sigma) &= F(E, \varepsilon, \sigma) - (f_1, \lambda(x, 0))_\varepsilon - ((\partial_t E, \partial_t \lambda))_\varepsilon - (f_0, \lambda(x, 0))_\sigma \\
&\quad - ((E, \partial_t \lambda))_\sigma + ((\nabla E, \nabla \lambda)) + ((\nabla \cdot (\varepsilon - 1)E, \nabla \cdot \lambda)) + ((\partial_t J, \lambda)) \\
&= F(E, \varepsilon, \sigma) + (\partial_t E, \lambda)_\varepsilon|_{t=0} - ((\partial_t E, \partial_t \lambda))_\varepsilon + (E, \lambda)_\sigma|_{t=0} \\
&\quad - ((E, \partial_t \lambda))_\sigma - \langle \langle \partial_n E, \lambda \rangle \rangle + ((\nabla E, \nabla \lambda)) - \langle \langle \nabla \cdot (\varepsilon - 1)E, n \cdot \lambda \rangle \rangle \\
&\quad + ((\nabla \cdot (\varepsilon - 1)E, \nabla \cdot \lambda)) + ((\partial_t J, \lambda)) \\
&= F(E, \varepsilon, \sigma) + ((\varepsilon \partial_t E + \sigma \partial_t E - \Delta E - \nabla \nabla \cdot (\varepsilon - 1)E + \partial_t J, \lambda)),
\end{aligned} \tag{3.5}$$

which holds for all  $\lambda \in H_\lambda^1$  and all  $E \in H_E^1 \cap H^2(\Omega_T)$  with homogeneous Neumann conditions.  $\square$

*Remark:* One can easily see that if  $E := E(\varepsilon, \sigma) \in H_E^1$  is a weak solution to the forward problem we have  $L(E, \lambda, \varepsilon, \sigma) = F(E, \varepsilon, \sigma)$  for all  $(E, \lambda, \varepsilon, \sigma) \in U$ .

To minimize  $L$  we look for stationary points  $u = (E, \lambda, \varepsilon, \sigma)$  such that for all  $\bar{u} = (\bar{E}, \bar{\lambda}, \bar{\varepsilon}, \bar{\sigma})$

$$L'(u; \bar{u}) = 0, \tag{3.6}$$

where  $L'$  is the Fréchet derivative of  $L$ . The statement above is equivalent to

$$L'(u; \bar{u}) = \left( \frac{\partial L}{\partial E}(u; \bar{E}), \frac{\partial L}{\partial \lambda}(u; \bar{\lambda}), \frac{\partial L}{\partial \varepsilon}(u; \bar{\varepsilon}), \frac{\partial L}{\partial \sigma}(u; \bar{\sigma}) \right) = 0. \tag{3.7}$$

**Lemma 3.2.** *The optimality conditions (3.7) in the weak form are given by following expressions:*

$$\begin{aligned}
\frac{\partial L}{\partial E}(u; \bar{E}) &= \langle \langle E - \bar{E}_{\text{obs}}, \bar{E} \rangle \rangle_{\Gamma_T} - ((\partial_t \bar{E}, \partial_t \lambda))_\varepsilon - ((\bar{E}, \partial_t \lambda))_\sigma + ((\nabla \bar{E}, \nabla \lambda)) \\
&\quad + ((\nabla \cdot (\varepsilon - 1)\bar{E}, \nabla \cdot \lambda)) = 0,
\end{aligned} \tag{3.8}$$

$$\begin{aligned}
\frac{\partial L}{\partial \lambda}(u; \bar{\lambda}) &= -(f_1, \bar{\lambda}(x, 0))_\varepsilon - ((\partial_t E, \partial_t \bar{\lambda}))_\varepsilon - (f_0, \bar{\lambda}(x, 0))_\sigma - ((E, \partial_t \bar{\lambda}))_\sigma \\
&\quad + ((\nabla E, \nabla \bar{\lambda})) + ((\nabla \cdot (\varepsilon - 1)E, \nabla \cdot \bar{\lambda})) + ((\partial_t J, \bar{\lambda})) = 0,
\end{aligned} \tag{3.9}$$

$$\frac{\partial L}{\partial \varepsilon}(u; \bar{\varepsilon}) = \gamma_\varepsilon(\varepsilon - \varepsilon^0, \bar{\varepsilon}) - (\bar{\varepsilon} f_1, \lambda(x, 0)) - ((\bar{\varepsilon} \partial_t E, \partial_t \lambda)) + ((\nabla \cdot \bar{\varepsilon} E, \nabla \cdot \lambda)) = 0, \tag{3.10}$$

$$\frac{\partial L}{\partial \sigma}(u; \bar{\sigma}) = \gamma_\sigma(\sigma - \sigma^0, \bar{\sigma}) - (\bar{\sigma} f_0, \lambda(x, 0)) - ((\bar{\sigma} E, \partial_t \lambda)) = 0. \tag{3.11}$$

*Proof.* To find the Fréchet derivative (3.7) of the Lagrangian (3.4) we consider  $L(u + \bar{u}) - L(u) \forall \bar{u} \in U$  and single out the linear part of the obtained equality with respect to  $\bar{u}$ . In our derivation of the Fréchet derivative we assume that all functions  $u = (E, \lambda, \varepsilon, \sigma) \in U$  in the Lagrangian (3.4) can be varied independently on each other called all-at-once approach.

Let us start first with derivation of the derivative with respect to  $E$ . Firstly, we can write

$$\begin{aligned} L(E + \bar{E}, \lambda, \varepsilon, \sigma) &= F(E + \bar{E}, \varepsilon, \sigma) - (f_1, \lambda(x, 0))_\varepsilon - ((\partial_t(E + \bar{E}), \partial_t \lambda))_\varepsilon \\ &\quad - (f_0, \lambda(x, 0))_\sigma - ((E + \bar{E}), \partial_t \lambda)_\sigma + ((\nabla(E + \bar{E}), \nabla \lambda)) \\ &\quad + ((\nabla \cdot (\varepsilon - 1)(E + \bar{E}), \nabla \cdot \lambda)) + ((\partial_t J, \lambda)). \end{aligned} \quad (3.12)$$

Here we note that for the Tikhonov functional we have:

$$\begin{aligned} F(E + \bar{E}, \varepsilon, \sigma) &= \frac{1}{2} \|E - \tilde{E}_{\text{obs}} + \bar{E}\|_{\Gamma_T}^2 + \frac{\gamma_\varepsilon}{2} \|\varepsilon - \varepsilon^0\|^2 + \frac{\gamma_\sigma}{2} \|\sigma - \sigma^0\|^2 \\ &= \frac{1}{2} \|E - \tilde{E}_{\text{obs}}\|_{\Gamma_T}^2 + \langle (E - \tilde{E}_{\text{obs}}, \bar{E}) \rangle_{\Gamma_T} + \frac{1}{2} \|\bar{E}\|_{\Gamma_T}^2 + \frac{\gamma_\varepsilon}{2} \|\varepsilon - \varepsilon^0\|^2 \\ &\quad + \frac{\gamma_\sigma}{2} \|\sigma - \sigma^0\|^2 = F(E, \varepsilon, \sigma) + \langle (E - \tilde{E}_{\text{obs}}, \bar{E}) \rangle_{\Gamma_T} + \frac{1}{2} \|\bar{E}\|_{\Gamma_T}^2. \end{aligned} \quad (3.13)$$

Inserting in (3.12) instead of  $F(E + \bar{E}, \varepsilon, \sigma)$  the right hand side of (3.13) we get:

$$\begin{aligned} L(E + \bar{E}, \lambda, \varepsilon, \sigma) &= F(E, \varepsilon, \sigma) + \langle (E - \tilde{E}_{\text{obs}}, \bar{E}) \rangle_{\Gamma_T} + \frac{1}{2} \|\bar{E}\|_{\Gamma_T}^2 \\ &\quad - (f_1, \lambda(x, 0))_\varepsilon - ((\partial_t(E + \bar{E}), \partial_t \lambda))_\varepsilon \\ &\quad - (f_0, \lambda(x, 0))_\sigma - ((E + \bar{E}), \partial_t \lambda)_\sigma + ((\nabla(E + \bar{E}), \nabla \lambda)) \\ &\quad + ((\nabla \cdot (\varepsilon - 1)(E + \bar{E}), \nabla \cdot \lambda)) + ((\partial_t J, \lambda)). \end{aligned} \quad (3.14)$$

Thus, if we separate the terms with  $\bar{E}$  in (3.14) and recognize terms corresponding to the Lagrangian  $L(E, \lambda, \varepsilon, \sigma)$  we can rewrite it as

$$\begin{aligned} L(E + \bar{E}, \lambda, \varepsilon, \sigma) &= L(E, \lambda, \varepsilon, \sigma) + \langle (E - \tilde{E}_{\text{obs}}, \bar{E}) \rangle_{\Gamma_T} - ((\partial_t \bar{E}, \partial_t \lambda))_\varepsilon \\ &\quad - ((\bar{E}, \partial_t \lambda))_\sigma + ((\nabla \bar{E}, \nabla \lambda)) + ((\nabla \cdot (\varepsilon - 1)\bar{E}, \nabla \cdot \lambda)) + \frac{1}{2} \|\bar{E}\|_{\Gamma_T}^2 \\ &= L(E, \lambda, \varepsilon, \sigma) + \frac{\partial L}{\partial \bar{E}}(E, \lambda, \varepsilon, \sigma; \bar{E}) + \mathcal{O}(\|\bar{E}\|^2). \end{aligned}$$

Now, considering  $L(E + \bar{E}, \lambda, \varepsilon, \sigma) - L(E, \lambda, \varepsilon, \sigma)$  and neglecting  $\mathcal{O}(\|\bar{E}\|^2)$  we get optimality condition (3.8).

The three other derivatives are approached very similarly. The derivative with respect to  $\lambda$  is simply a case of linearity of gradients and integrals,

$$\begin{aligned} L(E, \lambda + \bar{\lambda}, \varepsilon, \sigma) &= F(E, \varepsilon, \sigma) - (f_1, (\lambda + \bar{\lambda})(x, 0))_\varepsilon - ((\partial_t E, \partial_t (\lambda + \bar{\lambda})))_\varepsilon \\ &\quad - (f_0, (\lambda + \bar{\lambda})(x, 0))_\sigma - ((E, \partial_t (\lambda + \bar{\lambda})))_\sigma + ((\nabla E, \nabla (\lambda + \bar{\lambda}))) \\ &\quad + ((\nabla \cdot (\varepsilon - 1)E, \nabla \cdot (\lambda + \bar{\lambda}))) + ((\partial_t J, (\lambda + \bar{\lambda}))) \\ &= L(E, \lambda, \varepsilon, \sigma) - (f_1, \bar{\lambda}(x, 0))_\varepsilon - ((\partial_t E, \partial_t \bar{\lambda}))_\varepsilon - (f_0, \bar{\lambda}(x, 0))_\sigma \\ &\quad - ((E, \partial_t \bar{\lambda}))_\sigma + ((\nabla E, \nabla \bar{\lambda})) + ((\nabla \cdot (\varepsilon - 1)E, \nabla \cdot \bar{\lambda})) + ((\partial_t J, \bar{\lambda})) \\ &= L(E, \lambda, \varepsilon, \sigma) + \frac{\partial L}{\partial \lambda}(E, \lambda, \varepsilon, \sigma; \bar{\lambda}) + \mathcal{O}(\|\bar{\lambda}\|^2). \end{aligned}$$

Considering now  $L(E, \lambda + \bar{\lambda}, \varepsilon, \sigma) - L(E, \lambda, \varepsilon, \sigma)$  and neglecting  $\mathcal{O}(\|\bar{\lambda}\|^2)$  we get optimality condition (3.9).

For the derivative with respect to  $\varepsilon$  we have some second order terms from  $F$ , and we get:

$$\begin{aligned}
L(E, \lambda, \varepsilon + \bar{\varepsilon}, \sigma) &= F(E, \varepsilon + \bar{\varepsilon}, \sigma) - ((\varepsilon + \bar{\varepsilon})f_1, \lambda(x, 0)) - ((\varepsilon + \bar{\varepsilon})\partial_t E, \partial_t \lambda) \\
&\quad - (f_0, \lambda(x, 0))_\sigma - ((E, \partial_t \lambda))_\sigma + ((\nabla E, \nabla \lambda)) \\
&\quad + ((\nabla \cdot ((\varepsilon + \bar{\varepsilon}) - 1)E, \nabla \cdot \lambda)) + ((\partial_t J, \lambda)) \\
&= \frac{1}{2} \|E - \bar{E}_{\text{obs}}\|_{\Gamma_T}^2 + \frac{\gamma_\varepsilon}{2} \|(\varepsilon + \bar{\varepsilon}) - \varepsilon^0\|^2 + \frac{\gamma_\sigma}{2} \|\sigma - \sigma^0\|^2 \\
&\quad - (f_1, \lambda(x, 0))_\varepsilon - ((\partial_t E, \partial_t \lambda))_\varepsilon - (f_0, \lambda(x, 0))_\sigma - ((E, \partial_t \lambda))_\sigma \\
&\quad + ((\nabla E, \nabla \lambda)) + ((\nabla \cdot (\varepsilon - 1)E, \nabla \cdot \lambda)) + ((\partial_t J, \lambda)) \\
&\quad - (\bar{\varepsilon}f_1, \lambda(x, 0)) - ((\bar{\varepsilon}\partial_t E, \partial_t \lambda)) + ((\nabla \cdot \bar{\varepsilon}E, \nabla \cdot \lambda)) \\
&= L(E, \lambda, \varepsilon, \sigma) + \gamma_\varepsilon(\varepsilon - \varepsilon^0, \bar{\varepsilon}) - (\bar{\varepsilon}f_1, \lambda(x, 0)) - ((\bar{\varepsilon}\partial_t E, \partial_t \lambda)) \\
&\quad + ((\nabla \cdot \bar{\varepsilon}E, \nabla \cdot \lambda)) + \frac{\gamma_\varepsilon}{2} \|\bar{\varepsilon}\|^2 \\
&= L(E, \lambda, \varepsilon, \sigma) + \frac{\partial L}{\partial \varepsilon}(E, \lambda, \varepsilon, \sigma; \bar{\varepsilon}) + \mathcal{O}(\|\bar{\varepsilon}\|^2).
\end{aligned}$$

Considering now  $L(E, \lambda, \varepsilon + \bar{\varepsilon}, \sigma) - L(E, \lambda, \varepsilon, \sigma)$  and neglecting  $\mathcal{O}(\|\bar{\varepsilon}\|^2)$  we get optimality condition (3.10).

The derivation of the derivative with respect to  $\sigma$  is very similar, thus we omit some steps and write:

$$\begin{aligned}
L(E, \lambda, \varepsilon, \sigma + \bar{\sigma}) &= F(E, \varepsilon, \sigma + \bar{\sigma}) - (f_1, \lambda(x, 0))_\varepsilon - ((\partial_t E, \partial_t \lambda))_\varepsilon - ((\sigma + \bar{\sigma})f_0, \lambda(x, 0)) \\
&\quad - (((\sigma + \bar{\sigma})E, \partial_t \lambda)) + ((\nabla E, \nabla \lambda)) + ((\nabla \cdot (\varepsilon - 1)E, \nabla \cdot \lambda)) + ((\partial_t J, \lambda)) \\
&= L(E, \lambda, \varepsilon, \sigma) + \gamma_\sigma(\sigma - \sigma^0, \bar{\sigma}) - (\bar{\sigma}f_0, \lambda(x, 0)) - ((\bar{\sigma}E, \partial_t \lambda)) + \frac{\gamma_\sigma}{2} \|\bar{\sigma}\|^2 \\
&= L(E, \lambda, \varepsilon, \sigma) + \frac{\partial L}{\partial \sigma}(E, \lambda, \varepsilon, \sigma; \bar{\sigma}) + \mathcal{O}(\|\bar{\sigma}\|^2).
\end{aligned}$$

Considering now  $L(E, \lambda, \varepsilon, \sigma + \bar{\sigma}) - L(E, \lambda, \varepsilon, \sigma)$  and neglecting  $\mathcal{O}(\|\bar{\sigma}\|^2)$  we get the final optimality condition (3.11). □

It is quite simple to deduce that the optimality condition  $\frac{\partial L}{\partial \lambda}(u; \bar{\lambda}) = 0$  for all  $\bar{\lambda} \in H_\lambda^1$  is equivalent to the weak formulation of the forward problem, and the optimality condition  $\frac{\partial L}{\partial \bar{E}}(u; \bar{E}) = 0$  for all  $\bar{E} \in H_0^1$  also describes the *adjoint problem*.

Interpreting the Fréchet derivative as a weak formulation we want to find  $\lambda \in H^1(\Omega_T)$  such that

$$\begin{cases} \varepsilon \partial_t \lambda - \sigma \partial_t \lambda - \Delta \lambda - (\varepsilon - 1) \nabla \nabla \cdot \lambda = 0 & \text{for } (x, t) \in \Omega_T, & (3.15a) \\ \lambda(x, T) = \partial_t \lambda(x, T) = 0 & \text{for } x \in \Omega, & (3.15b) \\ \partial_n \lambda = -(E - \bar{E}_{\text{obs}}) & \text{for } (x, t) \in \Gamma_T. & (3.15c) \end{cases}$$

Note that this problem is solved backwards in time, thus the termination conditions and the sign swapped time derivatives compared to the forward problem.

## 4 Stability analysis for the forward and adjoint problems

In this section we will present stability estimates for the forward problem as well as the adjoint problem. We refer to [31] for general approach of derivation of stability estimates for PDEs. The proof of the forward problem's stability is derived in [8].

**Theorem 4.1.** *Assume  $\varepsilon \in C_\varepsilon$  and  $\sigma \in C_\sigma$ . Let  $\Omega \subset \mathbb{R}^3$  be a bounded domain with the piecewise smooth boundary  $\partial\Omega$ . For any  $t \in (0, T)$  let  $\Omega_t = \Omega \times (0, t)$  and  $\Gamma_t = \Gamma \times (0, t)$ . Suppose that there exists a solution  $E \in H^2(\Omega_T)$  of the model problem (2.8a–c). Then the vector  $E$  is unique and there exists a constant  $C = C(\|\varepsilon\|_{C^2(\Omega)}, \|\sigma\|, t)$  such that the following energy estimate holds true:*

$$\begin{aligned} |||E(t)|||^2 &:= \|\partial_t E(t)\|_\varepsilon^2 + \|E(t)\|_\sigma^2 + \|\nabla E(t)\|^2 + \|\nabla \cdot E(t)\|_{\varepsilon^{-1}}^2 \\ &\leq C \left[ \int_t^T \|\partial_t J(\tau)\|^2 d\tau + \|f_1\|_\varepsilon^2 + \|\nabla f_0\|^2 + \|f_0\|_\sigma^2 + \|\nabla \cdot f_0\|_{\varepsilon^{-1}}^2 \right]. \end{aligned} \quad (4.1)$$

The adjoint stability looks quite similar to the forward stability, both in terms of statement and proof. Thus we use the same ideas here for the proof as in [8].

**Theorem 4.2.** *Assume  $\varepsilon \in C_\varepsilon$  and  $\sigma \in C_\sigma$  holds. Let  $\Omega \subset \mathbb{R}^3$  be a bounded domain with the piecewise smooth boundary  $\partial\Omega$ . For any  $t \in (t, T)$  let  $\Omega_t = \Omega \times (t, T)$  and  $\Gamma_t = \Gamma \times (t, T)$ . Suppose that there exists a solution  $\lambda \in H^2(\Omega_T)$  of the adjoint problem (3.15a–c). Then the vector  $\lambda$  is unique and there exists a constant  $C = C(\|\varepsilon\|_{C^2}, t)$  such that the following energy estimate holds true:*

$$|||\lambda(t)|||^2 \leq C \|E - \tilde{E}_{\text{obs}}\|_{\Gamma_T}^2 \quad (4.2)$$

*Proof.* We begin our proof by multiplying (3.15a) by  $2\partial_t \lambda$  and integrate over  $\Omega_t$

$$((\varepsilon \partial_{tt} \lambda - \sigma \partial_t \lambda - \Delta \lambda - (\varepsilon - 1) \nabla \nabla \cdot \lambda, 2\partial_t \lambda))_{\Omega_t} = 0,$$

or equivalently and by naming the terms

$$\begin{aligned} I_1 + I_2 + I_3 + I_4 &:= 2((\partial_{tt} \lambda, \partial_t \lambda))_{\varepsilon, \Omega_t} - 2\|\partial_t \lambda\|_{\sigma, \Omega_t}^2 - 2((\Delta \lambda, \partial_t \lambda))_{\Omega_t} \\ &\quad - 2((\nabla \nabla \cdot \lambda, \partial_t \lambda))_{\varepsilon^{-1}, \Omega_t} = 0. \end{aligned}$$

We will estimate these terms one by one. First, by using integration by parts in time we have

$$I_1 = 2((\partial_{tt} \lambda, \partial_t \lambda))_{\varepsilon, \Omega_t} = \partial_t \|\partial_t \lambda\|_{\varepsilon, \Omega_t}^2 = \|\partial_t \lambda\|_\varepsilon^2 \Big|_{\tau=t}^T = -\|\partial_t \lambda(t)\|_\varepsilon^2,$$

where we made use of the chain rule and the finality conditions put on  $\lambda$ . Before we show an upper bound for  $I_2$ , we note that

$$\sqrt{\sigma} \lambda(t) = \sqrt{\sigma} \lambda(T) + \int_T^t \sqrt{\sigma} \partial_t \lambda(\tau) d\tau = - \int_t^T \sqrt{\sigma} \partial_t \lambda(\tau) d\tau,$$

By squaring both sides and integrating over  $\Omega$  we arrive at

$$\|\lambda(t)\|_{\sigma}^2 \leq \|\partial_t \lambda\|_{\sigma, \Omega_t}^2$$

and thus

$$I_2 = -2\|\partial_t \lambda\|_{\sigma, \Omega_t}^2 = -\|\partial_t \lambda\|_{\sigma, \Omega_t}^2 - \|\partial_t \lambda\|_{\sigma, \Omega_t}^2 \leq -\|\lambda(t)\|_{\sigma}^2 - \|\partial_t \lambda\|_{\sigma, \Omega_t}^2.$$

For estimation of  $I_3$  we simply integrate by parts,

$$\begin{aligned} I_3 &= -2((\Delta \lambda, \partial_t \lambda))_{\Omega_t} \\ &= -2((\partial_n \lambda, \partial_t \lambda))_{\Gamma_t} + 2((\nabla \lambda, \nabla \partial_t \lambda))_{\Omega_t} \\ &= 2\langle E - \tilde{E}_{\text{obs}}, \partial_t \lambda \rangle + \partial_t \|\nabla \lambda\|_{\Omega_t}^2 \\ &\leq \|E - \tilde{E}_{\text{obs}}\|_{\Gamma_t}^2 + \|\partial_t \lambda\|_{\Gamma_t}^2 + \|\nabla \lambda\|_{\Omega_t}^2|_{\tau=t} \\ &= \|E - \tilde{E}_{\text{obs}}\|_{\Gamma_t}^2 + \|\partial_t \lambda\|_{\Gamma_t}^2 - \|\nabla \lambda(t)\|^2, \end{aligned}$$

where we used that  $2\langle E - \tilde{E}_{\text{obs}}, \partial_t \lambda \rangle \leq \|E - \tilde{E}_{\text{obs}}\|_{\Gamma_t}^2 + \|\partial_t \lambda\|_{\Gamma_t}^2$ .

We use a similar approach to estimate  $I_4$ .

$$\begin{aligned} I_4 &= -2((\nabla \nabla \cdot \lambda, \partial_t \lambda))_{\varepsilon-1, \Omega_t} \\ &= -2((\nabla \cdot \lambda, \partial_t \lambda \cdot n))_{\varepsilon-1, \Gamma_t} + 2((\nabla \cdot \lambda, \nabla \cdot (\varepsilon - 1) \partial_t \lambda))_{\Omega_t} \\ &= 2((\nabla \cdot \lambda, (\varepsilon - 1) \nabla \cdot \partial_t \lambda + \nabla \varepsilon \cdot \partial_t \lambda))_{\Omega_t} \\ &= \partial_t \|\nabla \cdot \lambda\|_{\varepsilon-1, \Omega_t}^2 + 2((\nabla \cdot \lambda, \nabla \varepsilon \cdot \partial_t \lambda))_{\Omega_t} \\ &= \|\nabla \cdot \lambda(t)\|_{\varepsilon-1}^2|_{\tau=t} + 2((\nabla \cdot \lambda, \nabla \varepsilon \cdot \partial_t \lambda))_{\Omega_t}. \\ &= -\|\nabla \cdot \lambda(t)\|_{\varepsilon-1}^2 + 2((\nabla \cdot \lambda, \nabla \varepsilon \cdot \partial_t \lambda))_{\Omega_t}. \end{aligned}$$

Finally, collecting all terms in estimates for  $I_1, I_2, I_3, I_4$  and adding a new positive term  $\|\partial_t \lambda\|_{\Omega_t}^2$  we get:

$$\begin{aligned} 0 &= I_1 + I_2 + I_3 + I_4 \\ &\leq -\|\partial_t \lambda(t)\|_{\varepsilon}^2 - \|\lambda(t)\|_{\sigma}^2 - \|\partial_t \lambda\|_{\sigma, \Omega_t}^2 - \|\nabla \lambda(t)\|^2 - \|\nabla \cdot \lambda(t)\|_{\varepsilon-1}^2 \\ &\quad + 2((\nabla \cdot \lambda, \nabla \varepsilon \cdot \partial_t \lambda))_{\Omega_t} + \|E - \tilde{E}_{\text{obs}}\|_{\Gamma_t}^2 + \|\partial_t \lambda\|_{\Gamma_t}^2 + \|\partial_t \lambda\|_{\Omega_t}^2 \end{aligned} \quad (4.3)$$

Now, we gather all terms integrated over  $\Omega$  in (4.3) on the left hand side, together with additional term  $\|\partial_t \lambda\|_{\Gamma_t}^2$  which we will estimate later, and leave the rest of the terms on the right hand side in order to get the following estimate:

$$\begin{aligned} &\|\partial_t \lambda(t)\|_{\varepsilon}^2 + \|\lambda(t)\|_{\sigma}^2 + \|\nabla \lambda(t)\|^2 + \|\nabla \cdot \lambda(t)\|_{\varepsilon-1}^2 - \|\partial_t \lambda\|_{\Gamma_t}^2 \\ &\leq -\|\partial_t \lambda\|_{\sigma, \Omega_t}^2 + 2((\nabla \cdot \lambda, \nabla \varepsilon \cdot \partial_t \lambda))_{\Omega_t} + \|E - \tilde{E}_{\text{obs}}\|_{\Gamma_t}^2 + \|\partial_t \lambda\|_{\Omega_t}^2 \\ &\leq \|E - \tilde{E}_{\text{obs}}\|_{\Gamma_t}^2 + \|\nabla \varepsilon\|_{\infty}^2 \|\partial_t \lambda\|_{\Omega_t}^2 + \|\lambda\|_{\sigma, \Omega_t}^2 + \|\nabla \lambda\|_{\Omega_t}^2 + \|\nabla \cdot \lambda\|_{\Omega_t}^2, \end{aligned} \quad (4.4)$$

To estimate the term  $\|\partial_t \lambda\|_{\Gamma_t}^2$  in the left hand side of (4.4) we use the condition (3.15b), or  $\lambda(x, T) = 0$ , such that we can write

$$\lambda(x, t) = \lambda(x, T) + \int_T^t \partial_t \lambda(x, \tau) \, d\tau = - \int_t^T \partial_t \lambda(x, \tau) \, d\tau.$$

Now, squaring both sides of the above expression and integrating then over  $\Gamma$  we get

$$\|\lambda\|_{\Gamma}^2 \leq \|\partial_t \lambda\|_{\Gamma}^2,$$

which can be rewritten as

$$-\|\partial_t \lambda\|_{\Gamma}^2 \leq -\|\lambda\|_{\Gamma}^2. \quad (4.5)$$

Inserting the estimate (4.5) into the left hand side of (4.4), moving then the term  $\|\lambda\|_{\Gamma}^2$  to the right hand side of the obtained expression and estimating this term using the trace theorem

$$\|\lambda\|_{\Gamma}^2 \leq \int_{\Omega} (\lambda)^2 dx + \int_{\Omega} (\nabla \lambda)^2 dx = \|\lambda\|^2 + \|\nabla \lambda\|^2$$

we finally obtain:

$$\begin{aligned} \|\lambda(t)\|^2 &= \|\partial_t \lambda(t)\|_{\varepsilon}^2 + \|\lambda(t)\|_{\sigma}^2 + \|\nabla \lambda(t)\|^2 + \|\nabla \cdot \lambda(t)\|_{\varepsilon-1}^2 \\ &\leq \|\lambda\|_{\Gamma}^2 - \|\partial_t \lambda\|_{\sigma, \Omega_t}^2 + 2((\nabla \cdot \lambda, \nabla \varepsilon \cdot \partial_t \lambda)_{\Omega_t}) + \|E - \tilde{E}_{\text{obs}}\|_{\Gamma_t}^2 + \|\partial_t \lambda\|_{\Omega_t}^2 \\ &\leq \|E - \tilde{E}_{\text{obs}}\|_{\Gamma_t}^2 + C(\|\nabla \varepsilon\|_{\infty}^2 \|\partial_t \lambda\|_{\Omega_t}^2 + \|\lambda\|_{\sigma, \Omega_t}^2 + \|\nabla \lambda\|_{\Omega_t}^2 + \|\nabla \cdot \lambda\|_{\Omega_t}^2), \end{aligned} \quad (4.6)$$

or equivalently

$$\begin{aligned} \|\lambda(t)\|^2 &= \|\partial_t \lambda(t)\|_{\varepsilon}^2 + \|\lambda(t)\|_{\sigma-1}^2 + \|\nabla \lambda(t)\|^2 + \|\nabla \cdot \lambda(t)\|_{\varepsilon-1}^2 \\ &\leq \|E - \tilde{E}_{\text{obs}}\|_{\Gamma_t}^2 + C(\|\nabla \varepsilon\|_{\infty}^2 \|\partial_t \lambda\|_{\Omega_t}^2 + \|\lambda\|_{\sigma, \Omega_t}^2 + \|\nabla \lambda\|_{\Omega_t}^2 + \|\nabla \cdot \lambda\|_{\Omega_t}^2). \end{aligned} \quad (4.7)$$

Using

$$a(t) \leq b(t) + C \int_t^T a(\tau) d\tau$$

with

$$a(t) := \|\lambda(t)\|^2, \quad b(t) := \int_t^T \|E - \tilde{E}_{\text{obs}}\|_{\Gamma}^2, \quad C := C(\|\varepsilon\|_{C^2}).$$

An application of Grönwall's inequality to (4.7) yields the result given in (4.2).  $\square$

## 5 Mathematical analysis of optimization problem

To minimize our functional we will use gradient methods, so we begin to investigate the Fréchet derivative of  $J$  with respect to  $(\varepsilon, \sigma)$ . Before we do so we will have to establish mathematical analysis of our optimization problem.

Let us denote perturbations of coefficients  $\varepsilon, \sigma$  as  $\delta \varepsilon := \tilde{\varepsilon} - \varepsilon$ ,  $\delta \sigma := \tilde{\sigma} - \sigma$ , respectively.

**Lemma 5.1.** *The mapping  $(\varepsilon, \sigma) \rightarrow E(\varepsilon, \sigma)$  is Lipschitz continuous, i.e. for any  $\varepsilon, \varepsilon + \delta \varepsilon$  and  $\sigma, \sigma + \delta \sigma$  satisfying conditions (2.9) we have*

$$\|E(\varepsilon + \delta \varepsilon, \sigma + \delta \sigma) - E(\varepsilon, \sigma)\| \leq C(\|\delta \varepsilon\| + \|\delta \sigma\|), \quad (5.1)$$

where  $C = C(\tau, \|f_0\|, \|f_1\|) = \text{const.} > 0$ .

*Proof.* Let us introduce a new problem, similar to (2.8a–c) but for perturbed coefficients  $\tilde{\varepsilon} = \delta\varepsilon + \varepsilon$ ,  $\tilde{\sigma} = \delta\sigma + \sigma$ :

$$\begin{cases} \tilde{\varepsilon}\partial_{tt}\tilde{E} + \tilde{\sigma}\partial_t\tilde{E} - \Delta\tilde{E} + \nabla\nabla\cdot\tilde{E} - \nabla\nabla\cdot(\tilde{\varepsilon}\tilde{E}) = 0 & \text{for } (x,t) \in \Omega_T, & (5.2a) \\ \tilde{E}(x,0) = f_0, \partial_t\tilde{E}(x,0) = f_1 & \text{for } x \in \Omega, & (5.2b) \\ \partial_n\tilde{E} = 0 & \text{for } (x,t) \in \Gamma_T. & (5.2c) \end{cases}$$

If we now subtract (2.8a–c) from (8.1a–c), we get a third system

$$\begin{cases} \tilde{\varepsilon}\partial_{tt}\tilde{E} - \varepsilon\partial_{tt}E + \tilde{\sigma}\partial_t\tilde{E} - \sigma\partial_tE - \Delta\tilde{E} + \Delta E & (5.3a) \\ + \nabla\nabla\cdot\tilde{E} - \nabla\nabla\cdot E - \nabla\nabla\cdot(\tilde{\varepsilon}\tilde{E}) + \nabla\nabla\cdot(\varepsilon E) = 0 & \text{for } (x,t) \in \Omega_T, \\ \tilde{E}(x,0) - E(x,0) = 0, \partial_t\tilde{E}(x,0) - \partial_tE(x,0) = 0 & \text{for } x \in \Omega, & (5.3b) \\ \partial_n(\tilde{E} - E) = 0 & \text{for } (x,t) \in \Gamma_T. & (5.3c) \end{cases}$$

By introducing  $\mathbb{E} := \delta E = \tilde{E} - E$  and rearranging terms, we can rewrite (5.3a) as

$$\begin{aligned} & \tilde{\varepsilon}\partial_{tt}\tilde{E} - \varepsilon\partial_{tt}E + \tilde{\sigma}\partial_t\tilde{E} - \sigma\partial_tE - \Delta\tilde{E} + \Delta E + \nabla\nabla\cdot\tilde{E} - \nabla\nabla\cdot E - \nabla\nabla\cdot(\tilde{\varepsilon}\tilde{E}) + \nabla\nabla\cdot(\varepsilon E) \\ & = \tilde{\varepsilon}\partial_{tt}\tilde{E} - \varepsilon\partial_{tt}\tilde{E} + \varepsilon\partial_{tt}E - \varepsilon\partial_{tt}E + \tilde{\sigma}\partial_t\tilde{E} - \sigma\partial_t\tilde{E} + \sigma\partial_tE - \sigma\partial_tE - \Delta\tilde{E} + \Delta E \\ & + \nabla\nabla\cdot\tilde{E} - \nabla\nabla\cdot E - \nabla\nabla\cdot(\tilde{\varepsilon}\tilde{E}) - \nabla\nabla\cdot(\varepsilon\tilde{E}) + \nabla\nabla\cdot(\varepsilon\tilde{E}) + \nabla\nabla\cdot(\varepsilon E) \\ & = \delta\varepsilon\partial_{tt}\tilde{E} + \varepsilon\partial_{tt}\mathbb{E} + \delta\sigma\partial_t\tilde{E} + \sigma\partial_t\mathbb{E} - \Delta\mathbb{E} + \nabla\nabla\cdot\mathbb{E} - \nabla\nabla\cdot(\delta\varepsilon\tilde{E}) - \nabla\nabla\cdot(\varepsilon\mathbb{E}) = 0, \end{aligned}$$

and thus, the whole system can be rewritten as

$$\begin{cases} \varepsilon\partial_{tt}\mathbb{E} + \sigma\partial_t\mathbb{E} - \Delta\mathbb{E} + \nabla\nabla\cdot\mathbb{E} - \nabla\nabla\cdot(\varepsilon\mathbb{E}) & (5.4a) \\ = -\delta\varepsilon\partial_{tt}\tilde{E} - \delta\sigma\partial_t\tilde{E} - \nabla\nabla\cdot(\delta\varepsilon\tilde{E}) & \text{for } (x,t) \in \Omega_T, \\ \mathbb{E}(x,0) = 0, \partial_t\mathbb{E}(x,0) = 0 & \text{for } x \in \Omega, & (5.4b) \\ \partial_n\mathbb{E} = 0 & \text{for } (x,t) \in \Gamma_T. & (5.4c) \end{cases}$$

Applying stability estimate of the Theorem 4.1 for the problem (5.4a)–(5.4c) we can write that

$$\|\mathbb{E}\|^2 \leq C \int_0^T [\|\delta\varepsilon\|\|\partial_{tt}\tilde{E}\| + \|\delta\sigma\|\|\partial_t\tilde{E}\| + \|\nabla\nabla\cdot(\delta\varepsilon\tilde{E})\|]^2 d\tau. \quad (5.5)$$

For estimation of the term  $\|\nabla\nabla\cdot(\delta\varepsilon\tilde{E})\|$  in (5.5) one can use:

$$\|\nabla\nabla\cdot(\delta\varepsilon\tilde{E})\| = \|\nabla[\nabla\delta\varepsilon\tilde{E} + \delta\varepsilon\nabla\cdot\tilde{E}]\| \leq C \|\delta\varepsilon\|\|\tilde{E}\|. \quad (5.6)$$

Next, applying first Taylor's expansions

$$\begin{aligned} \tilde{E}(t+\tau) &= \tilde{E}(t) + \partial_t\tilde{E}(t)\tau + \partial_{tt}\tilde{E}(t)\frac{\tau^2}{2} + O(\tau^3), \\ \tilde{E}(t+\tau) &= \tilde{E}(t) + \partial_t\tilde{E}(t)\tau + O(\tau^2) \end{aligned} \quad (5.7)$$

for estimation of terms  $\partial_{tt}\tilde{E}$ ,  $\partial_t\tilde{E}$  in the right hand side of the estimate (5.5) such that

$$\begin{aligned} \partial_{tt}\tilde{E}(t) &\approx \frac{\tilde{E}(t+\tau) - 2\tilde{E}(t) + \tilde{E}(t-\tau)}{\tau^2}, \\ \partial_t\tilde{E}(t) &\approx \frac{\tilde{E}(t+\tau) - \tilde{E}(t-\tau)}{2\tau} \end{aligned} \quad (5.8)$$

and using after the Theorem 4.1 for the stability estimate of solution  $\tilde{E}$  of the problem (8.1a)-(8.1c) we obtain finally

$$\|\mathbb{E}\|^2 \leq C(\tau, \|f_0\|, \|f_1\|)(\|\delta\varepsilon\| + \|\delta\sigma\|)^2. \quad (5.9)$$

From (5.9) follows (5.1) and thus, the mapping  $(\varepsilon, \sigma) \rightarrow E(\varepsilon, \sigma)$  is Lipschitz continuous.  $\square$

**Lemma 5.2.** *The mapping  $(\varepsilon, \sigma) \rightarrow E(\varepsilon, \sigma)$  is Fréchet differentiable in the sense that for any  $\delta\varepsilon, \delta\sigma$  satisfying conditions (2.9) there exists a bounded linear operator  $A(\delta\varepsilon, \delta\sigma)$  such that*

$$\lim_{\|(\delta\varepsilon, \delta\sigma)\| \rightarrow 0} \frac{\|\tilde{E} - E - A(\delta\varepsilon, \delta\sigma)\|}{\|(\delta\varepsilon, \delta\sigma)\|} = 0.$$

Here,  $\|(\delta\varepsilon, \delta\sigma)\| := \|\delta\varepsilon\| + \|\delta\sigma\|$ ,  $A(\delta\varepsilon, \delta\sigma) = A(\delta\varepsilon) + A(\delta\sigma)$ , where  $A(\delta\varepsilon)$ ,  $A(\delta\sigma)$  are bounded linear operators.

*Proof.* Let us continue with the notation introduced in Lemma 5.1. Using  $\mathbb{E} = \tilde{E} - E$  we will let  $w := \tilde{E} - E - A(\delta\varepsilon, \delta\sigma) = \mathbb{E} - A(\delta\varepsilon, \delta\sigma)$ . We look for an operator  $A(\delta\varepsilon, \delta\sigma)$  such that

$$\lim_{\|(\delta\varepsilon, \delta\sigma)\| \rightarrow 0} \frac{\|w\|}{\|(\delta\varepsilon, \delta\sigma)\|} = 0,$$

where  $\tilde{E} := E(\varepsilon + \delta\varepsilon, \sigma + \delta\sigma)$ .

Now using  $\tilde{E} = \mathbb{E} + E$  we can rewrite (5.4a-c) as

$$\begin{cases} \varepsilon \partial_{tt} \mathbb{E} + \sigma \partial_t \mathbb{E} - \Delta \mathbb{E} + \nabla \nabla \cdot \mathbb{E} - \nabla \nabla \cdot (\varepsilon \mathbb{E}) & (5.10a) \\ = -\delta\varepsilon \partial_{tt} (\mathbb{E} + E) - \delta\sigma \partial_t (\mathbb{E} + E) - \nabla \nabla \cdot (\delta\varepsilon (\mathbb{E} + E)) & \text{for } (x, t) \in \Omega_T, \\ \mathbb{E}(x, 0) = 0, \partial_t \mathbb{E}(x, 0) = 0 & \text{for } x \in \Omega, & (5.10b) \\ \partial_n \mathbb{E} = 0 & \text{for } (x, t) \in \Gamma_T. & (5.10c) \end{cases}$$

Let  $u := A(\delta\varepsilon, \delta\sigma)$  and  $\mathbb{E} = w + u$ . This notation allows us rewrite the system above as

$$\begin{cases} \varepsilon \partial_{tt} (w + u) + \sigma \partial_t (w + u) - \Delta (w + u) \\ + \nabla \nabla \cdot (w + u) - \nabla \nabla \cdot (\varepsilon (w + u)) & (5.11a) \\ = -\delta\varepsilon \partial_{tt} (\mathbb{E} + E) - \delta\sigma \partial_t (\mathbb{E} + E) - \nabla \nabla \cdot (\delta\varepsilon (\mathbb{E} + E)) & \text{for } (x, t) \in \Omega_T, \\ \mathbb{E}(x, 0) = 0, \partial_t \mathbb{E}(x, 0) = 0 & \text{for } x \in \Omega, & (5.11b) \\ \partial_n \mathbb{E} = 0 & \text{for } (x, t) \in \Gamma_T, & (5.11c) \end{cases}$$

where  $w$  solves

$$\begin{cases} \varepsilon \partial_{tt} w + \sigma \partial_t w - \Delta w + \nabla \nabla \cdot w - \nabla \nabla \cdot (\varepsilon w) & (5.12a) \\ = -\delta\varepsilon \partial_{tt} \mathbb{E} - \delta\sigma \partial_t \mathbb{E} - \nabla \nabla \cdot (\delta\varepsilon \mathbb{E}) & \text{for } (x, t) \in \Omega_T, \\ w(x, 0) = 0, \partial_t w(x, 0) = 0 & \text{for } x \in \Omega, & (5.12b) \\ \partial_n w = 0 & \text{for } (x, t) \in \Gamma_T, & (5.12c) \end{cases}$$

and  $u$  solves

$$\begin{cases} \varepsilon \partial_{tt} u + \sigma \partial_t u - \Delta u + \nabla \nabla \cdot u - \nabla \nabla \cdot (\varepsilon u) & (5.13a) \\ = -\delta \varepsilon \partial_{tt} E - \delta \sigma \partial_t E - \nabla \nabla \cdot (\delta \varepsilon E) & \text{for } (x, t) \in \Omega_T, \\ u(x, 0) = 0, \partial_t u(x, 0) = 0 & \text{for } x \in \Omega, \\ \partial_n u = 0 & \text{for } (x, t) \in \Gamma_T. \end{cases} \quad (5.13b) \quad (5.13c)$$

Applying first the energy estimate derived in the Theorem 4.1 for the problem (5.12) for function  $w$  which will depend on  $\mathbb{E}$ , and then using the Lipschitz continuity estimate (5.1) for  $\mathbb{E}$ , will give us

$$\| \|w\| \|^2 \leq C \int_t^T [\| \delta \varepsilon \partial_{tt} \mathbb{E} \| + \| \delta \sigma \partial_t \mathbb{E} \| + \| \nabla \nabla \cdot (\delta \varepsilon \mathbb{E}) \|^2] d\tau \leq C (\| \delta \varepsilon \| + \| \delta \sigma \|^2). \quad (5.14)$$

Thus,

$$\lim_{\|(\delta \varepsilon, \delta \sigma)\| \rightarrow 0} \frac{\|w\|^2}{\|(\delta \varepsilon, \delta \sigma)\|} \leq \lim_{\|(\delta \varepsilon, \delta \sigma)\| \rightarrow 0} \frac{C(\| \delta \varepsilon \| + \| \delta \sigma \|^2)}{\|(\delta \varepsilon, \delta \sigma)\|} = 0,$$

which concludes the proof.  $\square$

**Theorem 5.3.** *The regularized functional*

$$F(\varepsilon, \sigma) := \frac{1}{2} \|E - \tilde{E}_{\text{obs}}\|_{\Gamma_T}^2 + \frac{\gamma_\varepsilon}{2} \|\varepsilon - \varepsilon^0\|^2 + \frac{\gamma_\sigma}{2} \|\sigma - \sigma^0\|^2 \quad (5.15)$$

is Fréchet differentiable and its gradient is

$$\begin{aligned} F'(\varepsilon, \sigma)(x) &:= F'(\varepsilon, \sigma)(\delta \varepsilon, \delta \sigma)(x) = \left[ \int_0^T \lambda (\delta \varepsilon \partial_{tt} E + \delta \sigma \partial_t E + \nabla \nabla \cdot (\delta \varepsilon E)) dt \right](x) \\ &+ [\gamma_\varepsilon (\varepsilon - \varepsilon^0) \delta \varepsilon + \gamma_\sigma (\sigma - \sigma^0) \delta \sigma](x) \end{aligned}$$

or in the weak form, after integration by parts and using initial conditions, the Fréchet derivative is written as:

$$\begin{aligned} F'(\varepsilon, \sigma)(x) &= -[f_1 \cdot \lambda|_{t=0} \delta \varepsilon - \int_0^T \partial_t E \cdot \partial_t \lambda \delta \varepsilon dt + \int_0^T \nabla \cdot \lambda \nabla \cdot (\delta \varepsilon E) dt \\ &- f_0 \cdot \lambda|_{t=0} \delta \sigma - \int_0^T E \cdot \partial_t \lambda \delta \sigma dt](x) \\ &+ [\gamma_\varepsilon (\varepsilon - \varepsilon^0) \delta \varepsilon + \gamma_\sigma (\sigma - \sigma^0) \delta \sigma](x) \end{aligned} \quad (5.16)$$

*Proof.* Recalling that  $\tilde{E} = \mathbb{E} + E$  we can compute:

$$\begin{aligned}
\delta F := F(\varepsilon + \delta\varepsilon, \sigma + \delta\sigma) - F(\varepsilon, \sigma) &= \frac{1}{2} \|\tilde{E} - \tilde{E}_{\text{obs}}\|_{\Gamma_T}^2 - \frac{1}{2} \|E - \tilde{E}_{\text{obs}}\|_{\Gamma_T}^2 \\
&\quad + \frac{\gamma_\varepsilon}{2} \|\varepsilon + \delta\varepsilon - \varepsilon^0\|^2 - \frac{\gamma_\varepsilon}{2} \|\varepsilon - \varepsilon^0\|^2 \\
&\quad + \frac{\gamma_\sigma}{2} \|\sigma + \delta\sigma - \sigma^0\|^2 - \frac{\gamma_\sigma}{2} \|\sigma - \sigma^0\|^2 \\
&= \frac{1}{2} \|\mathbb{E} + (E - \tilde{E}_{\text{obs}})\|_{\Gamma_T}^2 - \frac{1}{2} \|E - \tilde{E}_{\text{obs}}\|_{\Gamma_T}^2 \\
&\quad + \frac{\gamma_\varepsilon}{2} \|(\varepsilon - \varepsilon^0) + \delta\varepsilon\|^2 - \frac{\gamma_\varepsilon}{2} \|\varepsilon - \varepsilon^0\|^2 \\
&\quad + \frac{\gamma_\sigma}{2} \|(\sigma - \sigma^0) + \delta\sigma\|^2 - \frac{\gamma_\sigma}{2} \|\sigma - \sigma^0\|^2 \\
&= \frac{1}{2} \|\mathbb{E}\|_{\Gamma_T}^2 + \langle \mathbb{E}, E - \tilde{E}_{\text{obs}} \rangle_{\Gamma_T} \\
&\quad + \gamma_\varepsilon(\varepsilon - \varepsilon^0, \delta\varepsilon) + \gamma_\sigma(\sigma - \sigma^0, \delta\sigma) \\
&\quad + \frac{\gamma_\varepsilon}{2} \|\delta\varepsilon\|^2 + \frac{\gamma_\sigma}{2} \|\delta\sigma\|^2.
\end{aligned} \tag{5.17}$$

Let us write the variational formulation of the adjoint problem (3.15a) - (3.15c) for all  $\mathbb{E} \in H_\lambda^1$

$$(\langle \mathbb{E}, \varepsilon \partial_{tt} \lambda - \sigma \partial_t \lambda - \Delta \lambda + (1 - \varepsilon) \nabla \nabla \cdot \lambda \rangle) = 0,$$

and then perform integration by parts to get

$$\begin{aligned}
&\langle \langle E - \tilde{E}_{\text{obs}}, \mathbb{E} \rangle \rangle_{\Gamma_T} - ((\partial_t \mathbb{E}, \partial_t \lambda))_\varepsilon \\
&\quad - ((\mathbb{E}, \partial_t \lambda))_\sigma + ((\nabla \mathbb{E}, \nabla \lambda)) + ((\nabla \cdot (\varepsilon - 1) \mathbb{E}, \nabla \cdot \lambda)) = 0.
\end{aligned} \tag{5.18}$$

Then integrating by parts again (5.18) and noting that  $\mathbb{E}$  satisfy the problem (5.10a)–(5.10c) we get

$$\langle \langle E - \tilde{E}_{\text{obs}}, \mathbb{E} \rangle \rangle_{\Gamma_T} + ((\lambda, \varepsilon \partial_{tt} \mathbb{E} + \sigma \partial_t \mathbb{E} - \Delta \mathbb{E} + \nabla \nabla \cdot \mathbb{E} - \nabla \nabla \cdot (\varepsilon \mathbb{E}))) = 0.$$

We rewrite the last expression as

$$((\lambda, \varepsilon \partial_{tt} \mathbb{E} + \sigma \partial_t \mathbb{E} - \Delta \mathbb{E} + \nabla \nabla \cdot \mathbb{E} - \nabla \nabla \cdot (\varepsilon \mathbb{E}))) = -\langle \langle E - \tilde{E}_{\text{obs}}, \mathbb{E} \rangle \rangle_{\Gamma_T}. \tag{5.19}$$

Now replacing the term  $\langle \langle E - \tilde{E}_{\text{obs}}, \mathbb{E} \rangle \rangle_{\Gamma_T}$  in the expression (5.17) by the left hand side of the equation (5.19) we get:

$$\begin{aligned}
\delta F &= \frac{1}{2} \|\mathbb{E}\|_{\Gamma_T}^2 - ((\lambda, \varepsilon \partial_{tt} \mathbb{E} + \sigma \partial_t \mathbb{E} - \Delta \mathbb{E} + \nabla \nabla \cdot \mathbb{E} - \nabla \nabla \cdot (\varepsilon \mathbb{E}))) \\
&\quad + \gamma_\varepsilon(\varepsilon - \varepsilon^0, \delta\varepsilon) + \gamma_\sigma(\sigma - \sigma^0, \delta\sigma) \\
&\quad + \frac{\gamma_\varepsilon}{2} \|\delta\varepsilon\|^2 + \frac{\gamma_\sigma}{2} \|\delta\sigma\|^2 \\
&= \frac{1}{2} \|\mathbb{E}\|_{\Gamma_T}^2 - ((\lambda, -\delta\varepsilon \partial_{tt} \tilde{E} - \delta\sigma \partial_t \tilde{E} - \nabla \nabla \cdot (\delta\varepsilon \tilde{E})))
\end{aligned}$$

$$\begin{aligned}
& + \gamma_\varepsilon(\varepsilon - \varepsilon^0, \delta\varepsilon) + \gamma_\sigma(\sigma - \sigma^0, \delta\sigma) \\
& + \frac{\gamma_\varepsilon}{2} \|\delta\varepsilon\|^2 + \frac{\gamma_\sigma}{2} \|\delta\sigma\|^2.
\end{aligned}$$

Here, we have used first integration by parts and then definition of the right hand side in the problem (5.4a) - (5.4c).

Now we use again  $\tilde{E} = \mathbb{E} + E = \delta E + E$  to obtain

$$\begin{aligned}
\delta F &= \frac{1}{2} \|\delta E\|_{\Gamma_T}^2 - ((\lambda, -\delta\varepsilon\partial_{tt}\delta E - \delta\sigma\partial_t\delta E - \nabla\nabla \cdot (\delta\varepsilon\delta E))) \\
& - ((\lambda, -\delta\varepsilon\partial_{tt}E - \delta\sigma\partial_tE - \nabla\nabla \cdot (\delta\varepsilon E))) \\
& + \gamma_\varepsilon(\varepsilon - \varepsilon^0, \delta\varepsilon) + \gamma_\sigma(\sigma - \sigma^0, \delta\sigma) \\
& + \frac{\gamma_\varepsilon}{2} \|\delta\varepsilon\|^2 + \frac{\gamma_\sigma}{2} \|\delta\sigma\|^2.
\end{aligned}$$

We move all second order terms with  $\delta$ 's in the above expression to the right hand side by leaving all first order terms on the left hand side to get

$$\begin{aligned}
& \delta F + ((\lambda, -\delta\varepsilon\partial_{tt}E - \delta\sigma\partial_tE - \nabla\nabla \cdot (\delta\varepsilon E))) \\
& - \gamma_\varepsilon(\varepsilon - \varepsilon^0, \delta\varepsilon) - \gamma_\sigma(\sigma - \sigma^0, \delta\sigma) \\
& = \frac{1}{2} \|\delta E\|_{\Gamma_T}^2 - ((\lambda, -\delta\varepsilon\partial_{tt}\delta E - \delta\sigma\partial_t\delta E - \nabla\nabla \cdot (\delta\varepsilon\delta E))) \\
& + \frac{\gamma_\varepsilon}{2} \|\delta\varepsilon\|^2 + \frac{\gamma_\sigma}{2} \|\delta\sigma\|^2.
\end{aligned}$$

The expression above can be estimated now as

$$\begin{aligned}
& |\delta F + ((\lambda, -\delta\varepsilon\partial_{tt}E - \delta\sigma\partial_tE - \nabla\nabla \cdot (\delta\varepsilon E))) - \gamma_\varepsilon(\varepsilon - \varepsilon^0, \delta\varepsilon) - \gamma_\sigma(\sigma - \sigma^0, \delta\sigma)| \\
& \leq \mathcal{O}(\|\delta\varepsilon\|^2 + \|\delta\sigma\|^2)
\end{aligned}$$

which can be rewritten in the following form:

$$\begin{aligned}
& |F(\varepsilon + \delta\varepsilon, \sigma + \delta\sigma) - F(\varepsilon, \sigma) \\
& - [((\lambda, \delta\varepsilon\partial_{tt}E + \delta\sigma\partial_tE + \nabla\nabla \cdot (\delta\varepsilon E)) \\
& + \gamma_\varepsilon(\varepsilon - \varepsilon^0, \delta\varepsilon) + \gamma_\sigma(\sigma - \sigma^0, \delta\sigma))] \leq \mathcal{O}(\|\delta\varepsilon\|^2 + \|\delta\sigma\|^2).
\end{aligned} \tag{5.20}$$

Comparing now the definition of the Fréchet derivative written in the form

$$F(\varepsilon + \delta\varepsilon, \sigma + \delta\sigma) - F(\varepsilon, \sigma) - F'(\varepsilon, \sigma)(\delta\varepsilon, \delta\sigma) = \mathcal{O}(\|\delta\varepsilon\|^2 + \|\delta\sigma\|^2)$$

with the inequality (5.20) we observe that the functional  $F$  is Fréchet differentiable and the Fréchet derivative is given by

$$\begin{aligned}
F'(\varepsilon, \sigma)(x) &:= F'(\varepsilon, \sigma)(\delta\varepsilon, \delta\sigma)(x) = \left[ \int_0^T \lambda(\delta\varepsilon\partial_{tt}E + \delta\sigma\partial_tE + \nabla\nabla \cdot (\delta\varepsilon E)) dt \right](x) \\
& + [\gamma_\varepsilon(\varepsilon - \varepsilon^0)\delta\varepsilon + \gamma_\sigma(\sigma - \sigma^0)\delta\sigma](x)
\end{aligned}$$

or in the weak form, after integration by parts and using initial conditions for the model problem, the Fréchet derivative is written as:

$$\begin{aligned}
F'(\varepsilon, \sigma)(x) &= -[f_1 \cdot \lambda|_{t=0} \delta \varepsilon - \int_0^T \partial_t E \cdot \partial_t \lambda \delta \varepsilon dt + \int_0^T \nabla \cdot \lambda \nabla \cdot (\delta \varepsilon E) dt \\
&\quad - f_0 \cdot \lambda|_{t=0} \delta \sigma - \int_0^T E \cdot \partial_t \lambda \delta \sigma dt](x) \\
&\quad + [\gamma_\varepsilon(\varepsilon - \varepsilon^0) \delta \varepsilon + \gamma_\sigma(\sigma - \sigma^0) \delta \sigma](x)
\end{aligned} \tag{5.21}$$

□

**Lemma 5.4.** *Assume that the solution  $E(\varepsilon, \sigma)$  for the forward problem (2.8a) – (2.8c) and the solution  $\lambda(\varepsilon, \sigma)$  for the adjoint problem (3.15a) – (3.15c) are sufficiently stable, i.e. satisfy stability estimates derived in the Theorem 4.1 for the forward problem and in the Theorem 4.2 for the adjoint problem, respectively. Then the Fréchet derivative of the Tikhonov functional  $F(\varepsilon, \sigma)$  can be computed also via Fréchet derivative of the Lagrangian  $L$  as:*

$$F'(\varepsilon, \sigma) := F'(E(\varepsilon, \sigma), \varepsilon, \sigma) = \frac{\partial L}{\partial \varepsilon}(E(\varepsilon, \sigma), \lambda, \varepsilon, \sigma) + \frac{\partial L}{\partial \sigma}(E(\varepsilon, \sigma), \lambda, \varepsilon, \sigma). \tag{5.22}$$

where  $L$  is the Lagrangian.

*Proof.* Comparing the Fréchet derivative  $F'(\varepsilon, \sigma)$  in the weak form given by (5.21) with the Fréchet derivatives  $\frac{\partial L}{\partial \varepsilon}(E(\varepsilon, \sigma), \lambda, \varepsilon, \sigma)$ ,  $\frac{\partial L}{\partial \sigma}(E(\varepsilon, \sigma), \lambda, \varepsilon, \sigma)$  given by optimality conditions of the Lagrangian in (3.10), (3.11), respectively, and then taking them with  $\bar{\varepsilon} = \delta \varepsilon$ ,  $\bar{\sigma} = \delta \sigma$ , we obtain equality (5.22). □

## 6 Existence of minimizer

**Lemma 6.1.** *The following expression holds for the non-regularized Tikhonov functional  $F(\varepsilon, \sigma)$ :*

$$F(\varepsilon, \sigma) = F(\varepsilon_n, \sigma_n) - \frac{1}{2} \int_{\Gamma_T} (\delta E_n)^2 ds dt + \int_{\Gamma_T} [E(\varepsilon, \sigma) - \tilde{E}_{\text{obs}}] \delta E_n ds dt, \tag{6.1}$$

where  $\delta E_n := E(\varepsilon, \sigma) - E(\varepsilon_n, \sigma_n)$ .

*Proof.* We have:

$$\begin{aligned}
F(\varepsilon, \sigma) - F(\varepsilon_n, \sigma_n) &= \frac{1}{2} \int_{\Gamma_T} [E(\varepsilon, \sigma) - \tilde{E}_{\text{obs}}]^2 ds dt - \frac{1}{2} \int_{\Gamma_T} [E(\varepsilon_n, \sigma_n) - \tilde{E}_{\text{obs}}]^2 ds dt \\
&= \frac{1}{2} \int_{\Gamma_T} ([E(\varepsilon, \sigma) - \tilde{E}_{\text{obs}}]^2 - [E(\varepsilon_n, \sigma_n) - \tilde{E}_{\text{obs}}]^2) ds dt.
\end{aligned} \tag{6.2}$$

Let  $a = E(\varepsilon, \sigma)$ ,  $b = \tilde{E}_{\text{obs}}$ ,  $c = E(\varepsilon_n, \sigma_n)$ . Then we simplify

$$[E(\varepsilon, \sigma) - \tilde{E}_{\text{obs}}]^2 - [E(\varepsilon_n, \sigma_n) - \tilde{E}_{\text{obs}}]^2 = (a-b)^2 - (c-b)^2 \quad (6.3)$$

as follows:

$$\begin{aligned} (a-b)^2 - (c-b)^2 &= (a-b-(c-b))(a-b+(c-b)) = (a-c)(a-2b+c) \\ &= (a-c)((a+c)-2b) = (a-c)(a+c) - 2b(a-c). \end{aligned} \quad (6.4)$$

Substituting (6.4) into (6.3) and then to (6.10) we get:

$$\begin{aligned} F(\varepsilon, \sigma) - F(\varepsilon_n, \sigma_n) &= \frac{1}{2} \int_{\Gamma_T} (E(\varepsilon, \sigma) - E(\varepsilon_n, \sigma_n))(E(\varepsilon, \sigma) + E(\varepsilon_n, \sigma_n)) dsdt \\ &\quad - \int_{\Gamma_T} \tilde{E}_{\text{obs}}(E(\varepsilon, \sigma) - E(\varepsilon_n, \sigma_n)) dsdt. \end{aligned} \quad (6.5)$$

Let  $\delta E_n := E(\varepsilon, \sigma) - E(\varepsilon_n, \sigma_n)$ ;  $E = E(\varepsilon, \sigma)$ ,  $E_n = E(\varepsilon_n, \sigma_n)$ . Then from (6.5) it follows:

$$\begin{aligned} F(\varepsilon, \sigma) - F(\varepsilon_n, \sigma_n) &= \frac{1}{2} \int_{\Gamma_T} \delta E_n (E + E_n) dsdt - \int_{\Gamma_T} \tilde{E}_{\text{obs}} \delta E_n dsdt \\ &= \frac{1}{2} \int_{\Gamma_T} \delta E_n (E + E_n) dsdt - \int_{\Gamma_T} \tilde{E}_{\text{obs}} \delta E_n dsdt \\ &\quad + \int_{\Gamma_T} E \delta E_n dsdt - \int_{\Gamma_T} E \delta E_n dsdt \\ &= \frac{1}{2} \int_{\Gamma_T} \delta E_n E_n dsdt - \int_{\Gamma_T} \tilde{E}_{\text{obs}} \delta E_n dsdt \\ &\quad + \int_{\Gamma_T} E \delta E_n dsdt - \frac{1}{2} \int_{\Gamma_T} E \delta E_n dsdt \\ &= \int_{\Gamma_T} (E - \tilde{E}_{\text{obs}}) \delta E_n dsdt - \frac{1}{2} \int_{\Gamma_T} (E - E_n) \delta E_n dsdt \\ &= \int_{\Gamma_T} (E - \tilde{E}_{\text{obs}}) \delta E_n dsdt - \frac{1}{2} \int_{\Gamma_T} (\delta E_n)^2 dsdt, \end{aligned} \quad (6.6)$$

and thus, we obtained (6.1).  $\square$

**Theorem 6.2.** *Assume that conditions (2.9) for functions  $\varepsilon, \sigma$  holds true. Then there exists a unique minimizer of the non-regularized functional  $F(\varepsilon, \sigma)$ .*

*Proof.* Using the fact that the functional  $F(\varepsilon, \sigma)$  is bounded from below then there exists a minimizing sequences  $\{\varepsilon_n\} \in C_\varepsilon$ ,  $\{\sigma_n\} \in C_\sigma$  which converges weakly to admissible functions  $\varepsilon \in C_\varepsilon$ ,  $\sigma \in C_\sigma$ . By the Lemma 6.1 the following expression holds for the non regularized Tikhonov functional  $F(\varepsilon, \sigma)$ :

$$\begin{aligned} F(\varepsilon, \sigma) &= F(\varepsilon_n, \sigma_n) - \frac{1}{2} \int_{\Gamma_T} [\delta E_n]^2 dsdt \\ &\quad + \int_{\Gamma_T} [E(\varepsilon, \sigma) - \tilde{E}_{\text{obs}}] \delta E_n dsdt, \end{aligned} \quad (6.7)$$

where  $\delta E_n := E(\varepsilon, \sigma) - E(\varepsilon_n, \sigma_n)$ .

Taking  $\delta E_n := \mathbb{E}$  in (6.7) and using then (5.19) we get

$$\begin{aligned} F(\varepsilon, \sigma) &\leq F(\varepsilon_n, \sigma_n) - ((\lambda, \varepsilon \partial_{tt} \mathbb{E} + \sigma \partial_t \mathbb{E} - \Delta \mathbb{E} + \nabla \nabla \cdot \mathbb{E} - \nabla \nabla \cdot (\varepsilon \mathbb{E}))) \\ &= F(\varepsilon_n, \sigma_n) - ((\lambda, -\delta \varepsilon_n \partial_{tt} \tilde{E} - \delta \sigma_n \partial_t \tilde{E} - \nabla \nabla \cdot (\delta \varepsilon_n \tilde{E}))). \end{aligned} \quad (6.8)$$

Here, we have used definition of the right hand side in the problem (5.4a) - (5.4c).

By Hölder's inequality the term  $\int_0^T \lambda (-\delta \varepsilon_n \partial_{tt} \tilde{E} - \delta \sigma_n \partial_t \tilde{E} - \nabla \nabla \cdot (\delta \varepsilon_n \tilde{E})) dt \in L^2(\Omega)$ . Since  $\varepsilon_n \rightharpoonup \varepsilon$ ,  $\sigma_n \rightharpoonup \sigma$  in  $L^2(\Omega)$ , we get

$$((\lambda, -\varepsilon_n \partial_{tt} \tilde{E} - \sigma_n \partial_t \tilde{E} - \nabla \nabla \cdot (\varepsilon_n \tilde{E}))) \rightarrow ((\lambda, -\varepsilon \partial_{tt} \tilde{E} - \sigma \partial_t \tilde{E} - \nabla \nabla \cdot (\varepsilon \tilde{E}))) \quad \text{as } n \rightarrow \infty.$$

From the above expression follows that

$$F(\varepsilon, \sigma) \leq \liminf_{n \rightarrow \infty} F(\varepsilon_n, \sigma_n) \quad (6.9)$$

Further, since  $\varepsilon_n \rightharpoonup \varepsilon$ ,  $\sigma_n \rightharpoonup \sigma$  in  $L^2(\Omega)$ , it is also lower semi-continuous, what means that if

$$\begin{aligned} \|\varepsilon\|_{L^2(\Omega)} &\leq \liminf_{n \rightarrow \infty} \|\varepsilon_n\|_{L^2(\Omega)}, \\ \|\sigma\|_{L^2(\Omega)} &\leq \liminf_{n \rightarrow \infty} \|\sigma_n\|_{L^2(\Omega)}, \end{aligned}$$

then this implies that

$$F(\varepsilon, \sigma) \leq \liminf_{n \rightarrow \infty} F(\varepsilon_n, \sigma_n),$$

and hence  $F(\varepsilon, \sigma)$  is lower semi-continuous. From the Theorem 1.9.1.2 of [11] it also follows that the functional  $F(\varepsilon, \sigma)$  is locally strictly convex in the neighborhood of the minimizer  $(\varepsilon, \sigma)$ . Thus, using the generalized Weierstrass theorem (see [43], Theorem 2D), we conclude that the regularized functional  $F(\varepsilon, \sigma)$  has a unique minimizer what finishes our proof.  $\square$

**Lemma 6.3.** *The following expression holds for the regularized Tikhonov functional  $F(\varepsilon, \sigma)$ :*

$$\begin{aligned} F(\varepsilon, \sigma) &= F(\varepsilon_n, \sigma_n) - \frac{1}{2} \int_{\Gamma_T} (\delta E_n)^2 ds dt + \int_{\Gamma_T} [E(\varepsilon, \sigma) - \tilde{E}_{\text{obs}}] \delta E_n ds dt \\ &\quad - \frac{1}{2} \gamma_\varepsilon \int_{\Omega} (\delta \varepsilon_n)^2 dx + \gamma_\varepsilon \int_{\Omega} [\varepsilon - \varepsilon^0] \delta \varepsilon_n dx \\ &\quad - \frac{1}{2} \gamma_\sigma \int_{\Omega} (\delta \sigma_n)^2 dx + \gamma_\sigma \int_{\Omega} [\sigma - \sigma^0] \delta \sigma_n dx \end{aligned} \quad (6.10)$$

where  $\delta E_n := E(\varepsilon, \sigma) - E(\varepsilon_n, \sigma_n)$ ,  $\delta \varepsilon_n := \varepsilon - \varepsilon_n$ ,  $\delta \sigma_n := \sigma - \sigma_n$ .

*Proof.* In the proof we use Lemma 6.2 for the non-regularized Tikhonov functional to obtain expression (6.1). In the case of the regularized Tikhonov functional (3.1) we should estimate additional regularization terms appearing in the computation of  $F(\varepsilon, \sigma) - F(\varepsilon_n, \sigma_n)$ .

Thus, we first estimate the regularization terms for  $\varepsilon$  as follows. Let us take  $a = \varepsilon, b = \varepsilon^0, c = \varepsilon_n$  in (6.4) to obtain:

$$(\varepsilon - \varepsilon^0)^2 - (\varepsilon_n - \varepsilon^0)^2 = (\varepsilon - \varepsilon_n)(\varepsilon + \varepsilon_n) - 2\varepsilon^0(\varepsilon - \varepsilon_n) \quad (6.11)$$

and thus, denoting  $\delta\varepsilon_n := \varepsilon - \varepsilon_n$  we get:

$$\begin{aligned} \frac{1}{2}\gamma_\varepsilon \int_{\Omega} [(\varepsilon - \varepsilon^0)^2 - (\varepsilon_n - \varepsilon^0)^2] dx &= \frac{1}{2}\gamma_\varepsilon \int_{\Omega} [(\varepsilon - \varepsilon_n)(\varepsilon + \varepsilon_n) - 2\varepsilon^0(\varepsilon - \varepsilon_n)] dx \\ &= \frac{1}{2}\gamma_\varepsilon \int_{\Omega} [\delta\varepsilon_n(\varepsilon + \varepsilon_n) - 2\varepsilon^0\delta\varepsilon_n] dx + \gamma_\varepsilon \int_{\Omega} \varepsilon\delta\varepsilon_n dx - \gamma_\varepsilon \int_{\Omega} \varepsilon^0\delta\varepsilon_n dx \\ &= -\frac{1}{2}\gamma_\varepsilon \int_{\Omega} (\varepsilon - \varepsilon_n)\delta\varepsilon_n dx + \gamma_\varepsilon \int_{\Omega} (\varepsilon - \varepsilon^0)\delta\varepsilon_n dx \\ &= -\frac{1}{2}\gamma_\varepsilon \int_{\Omega} (\delta\varepsilon_n)^2 dx + \gamma_\varepsilon \int_{\Omega} (\varepsilon - \varepsilon^0)\delta\varepsilon_n dx. \end{aligned} \quad (6.12)$$

In a similar way we estimate terms for  $\sigma$ :

$$\begin{aligned} \frac{1}{2}\gamma_\sigma \int_{\Omega} [(\sigma - \sigma^0)^2 - (\sigma_n - \sigma^0)^2] dx &= \frac{1}{2}\gamma_\sigma \int_{\Omega} [(\sigma - \sigma_n)(\sigma + \sigma_n) - 2\sigma^0(\sigma - \sigma_n)] dx \\ &= \frac{1}{2}\gamma_\sigma \int_{\Omega} [\delta\sigma_n(\sigma + \sigma_n) - 2\sigma^0\delta\sigma_n] dx + \gamma_\sigma \int_{\Omega} \sigma\delta\sigma_n dx - \gamma_\sigma \int_{\Omega} \sigma^0\delta\sigma_n dx \\ &= -\frac{1}{2}\gamma_\sigma \int_{\Omega} (\sigma - \sigma_n)\delta\sigma_n dx + \gamma_\sigma \int_{\Omega} (\sigma - \sigma^0)\delta\sigma_n dx \\ &= -\frac{1}{2}\gamma_\sigma \int_{\Omega} (\delta\sigma_n)^2 dx + \gamma_\sigma \int_{\Omega} (\sigma - \sigma^0)\delta\sigma_n dx. \end{aligned} \quad (6.13)$$

Combining now (6.1) with (6.12),(6.13) we get (6.10).  $\square$

**Theorem 6.4.** *Assume that conditions (2.9) for functions  $\varepsilon, \sigma$  holds true. Then there exists a unique minimizer of the regularized functional  $F(\varepsilon, \sigma)$  given in (3.1).*

*Proof.* We use proof for the non-regularized functional noting that by the Lemma 6.3 the expression (6.10) holds for the regularized Tikhonov functional  $F(\varepsilon, \sigma)$ . Since  $\varepsilon_n \rightharpoonup \varepsilon, \sigma_n \rightharpoonup \sigma$  in  $L^2(\Omega)$ , we get then that the terms with  $\delta\varepsilon_n, \delta\sigma_n$  in (6.10) tends to zero as  $n \rightarrow \infty$ , as well as

$$\lim_{n \rightarrow \infty} ((\lambda, -\varepsilon_n \partial_{tt} \tilde{E} - \sigma_n \partial_t \tilde{E} - \nabla \nabla \cdot (\varepsilon_n \tilde{E}))) = ((\lambda, -\varepsilon \partial_{tt} \tilde{E} - \sigma \partial_t \tilde{E} - \nabla \nabla \cdot (\varepsilon \tilde{E}))).$$

Using these facts in (6.10) we get the inequality

$$F(\varepsilon, \sigma) \leq \lim_{n \rightarrow \infty} F(\varepsilon_n, \sigma_n).$$

The rest of the proof is the same as the proof following after (6.9).  $\square$

## 7 Algorithms for solution of inverse problem

In our numerical simulations we are using two different gradient-based algorithms: conjugate gradient algorithm (CGA) and adaptive CGA (ACGA). ACGA uses adaptive finite element method in space which significantly improves reconstructions of  $\varepsilon, \sigma$  obtained on the initially non-refined mesh using usual CGA - see details on this method in [5, 11, 13].

Let us define the following functions which are obtained from optimal conditions  $\frac{\partial L}{\partial \varepsilon}(u; \bar{\varepsilon}) = 0$  and  $\frac{\partial L}{\partial \sigma}(u; \bar{\sigma}) = 0$  derived in Lemma 3.2 and which we will use in the conjugate gradient algorithm (CGA):

$$g_\varepsilon(x) := [\gamma_\varepsilon(\varepsilon - \varepsilon^0) - \lambda(x, 0)f_1 - \int_0^T \partial_t \lambda \partial_t E \, dt + \int_0^T \nabla \cdot \lambda \nabla \cdot E \, dt](x), \quad (7.1)$$

$$g_\sigma(x) := [\gamma_\sigma(\sigma - \sigma^0) - f_0 \lambda(x, 0) - \int_0^T E \partial_t \lambda \, dt](x). \quad (7.2)$$

In (7.1) we have used that  $\nabla \cdot (\bar{\varepsilon}E) = \nabla \bar{\varepsilon}E + \bar{\varepsilon} \nabla \cdot E \approx \bar{\varepsilon} \nabla \cdot E$ .

Let  $\varepsilon^m$  and  $\sigma^m$  are the coefficients computed on the iteration  $m$  of the CGA, and  $E^m := E(\varepsilon^m, \sigma^m)(x, t)$ ,  $\lambda^m := \lambda(E^m, \varepsilon^m, \sigma^m)(x, t)$ ,  $g_\varepsilon^m := g_\varepsilon^m(x)$  and  $g_\sigma^m := g_\sigma^m(x)$  where  $E(\varepsilon^m, \sigma^m)$  and  $\lambda(E^m, \varepsilon^m, \sigma^m)$  are the solutions of the forward and adjoint problems, respectively. Algorithm 1 summarizes the conjugate gradient algorithm in continuous setting.

The main idea of the adaptive local mesh refinement used in ACGA is that the finite element mesh  $K_h$  constructed in the finite element domain  $\Omega_{\text{FEM}}$  should be refined in such elements  $K$  of  $K_h$  where both functions  $|h\varepsilon_h^M|, |h\sigma_h^M|$  achieve its maximum values at the final iteration  $M$  in CGA:

$$\begin{aligned} |h\varepsilon_h^M| &\geq \tilde{\beta}_\varepsilon \max_{K_h} |h\varepsilon_h^M|, \\ |h\sigma_h^M| &\geq \tilde{\beta}_\sigma \max_{K_h} |h\sigma_h^M|. \end{aligned} \quad (7.5)$$

Here, numbers  $\tilde{\beta}_\varepsilon \in (0, 1), \tilde{\beta}_\sigma \in (0, 1)$  should be chosen computationally depending on the results of reconstruction in CGA, and  $h = h(x)$  is a piecewise-constant mesh function representing the local diameter of the elements and is defined as ( see details in [30])

$$h|_K = h_K \quad \forall K \in K_h. \quad (7.6)$$

The mesh refinements recommendations (7.5) are based on a posteriori error estimates for the errors  $|\varepsilon - \varepsilon_h^M|, |\sigma - \sigma_h^M|$  in the reconstructed functions  $\varepsilon_h^M, \sigma_h^M$ , respectively. The proofs of a posteriori error estimates can be derived using technique of [11] and is topic of the ongoing research. Algorithm 2 summarizes an adaptive conjugate gradient algorithm in the discrete setting.

Note that we perform mesh refinements only in space and not in time to be able smoothly run the domain decomposition finite element/finite difference method for solutions of the forward and adjoint problems - see details of this method for our model problem in [5].

---

**Algorithm 1** Conjugate Gradient Algorithm (CGA): For iterations  $m = 0, \dots, M$  perform following steps.

---

- 1: Initialization: set  $m = 0$  and choose initial guesses  $\varepsilon^0, \sigma^0, \gamma_\varepsilon^0, \gamma_\sigma^0, \alpha_\varepsilon^0, \alpha_\sigma^0$ .
- 2: Calculate  $E^m, \lambda^m, g_\varepsilon^m$  and  $g_\sigma^m$ .
- 3: Update the dielectric permittivity as:

$$\begin{aligned}\varepsilon^{m+1} &:= \varepsilon^m + \alpha_\varepsilon^m d_\varepsilon^m, \\ d_\varepsilon^m &:= -g_\varepsilon^m + \beta_\varepsilon^m d_\varepsilon^{m-1}, \\ \beta_\varepsilon^m &:= \frac{\|g_\varepsilon^m\|^2}{\|g_\varepsilon^{m-1}\|^2},\end{aligned}$$

and the conductivity as:

$$\begin{aligned}\sigma^{m+1} &:= \sigma^m + \alpha_\sigma^m d_\sigma^m, \\ d_\sigma^m &:= -g_\sigma^m + \beta_\sigma^m d_\sigma^{m-1}, \\ \beta_\sigma^m &:= \frac{\|g_\sigma^m\|^2}{\|g_\sigma^{m-1}\|^2},\end{aligned}$$

where  $\alpha_\varepsilon^m, \alpha_\sigma^m$  are optimal step sizes in CGA with  $d_\varepsilon^0 := -g_\varepsilon^0, d_\sigma^0 := -g_\sigma^0$ .

- 4: Compute new optimal step-sizes as

$$\alpha_\varepsilon^{m+1} = -\frac{(g_\varepsilon^m, d_\varepsilon^m)}{\gamma_\varepsilon^m(d_\varepsilon^m, d_\varepsilon^m)}, \quad \alpha_\sigma^{m+1} = -\frac{(g_\sigma^m, d_\sigma^m)}{\gamma_\sigma^m(d_\sigma^m, d_\sigma^m)}. \quad (7.3)$$

- 5: Compute new regularization parameters iteratively for any  $p \in (0, 1)$  via rules of [4] as

$$\gamma_\varepsilon^{m+1} = \frac{\gamma_\varepsilon^0}{(m+1)^p}, \quad \gamma_\sigma^{m+1} = \frac{\gamma_\sigma^0}{(m+1)^p} \quad (7.4)$$

- 6: Terminate the algorithm if either  $\|\varepsilon^{m+1} - \varepsilon^m\| < \eta_\varepsilon^1$  or  $\|\sigma^{m+1} - \sigma^m\| < \eta_\sigma^1$ , or  $\|g_\varepsilon^m\| < \eta_\varepsilon^2$  or  $\|g_\sigma^m\| < \eta_\sigma^2$ , where  $\eta_\varepsilon^1, \eta_\varepsilon^2, \eta_\sigma^1$  and  $\eta_\sigma^2$  are tolerances chosen by the user. Otherwise, set  $m := m + 1$  and repeat the algorithm from step 2.
- 

## 8 Numerical examples

In this section we present two- and three-dimensional numerical tests for the reconstruction of both the dielectric permittivity and conductivity functions, which are used to assess the performance of the optimization-based CGA and ACGA algorithms introduced in Section 7.

All two-dimensional experiments are carried out using the CGA described in Section 7, with the corresponding code developed and tested in MATLAB. The three-dimensional experiments employ the ACGA from Section 7 and are implemented in

---

**Algorithm 2** Adaptive Conjugate Gradient Algorithm (ACGA): For mesh refinements  $k = 0, \dots, N$  perform the steps below.

---

- 1: Choose initial spatial mesh  $K_{h0}$  in  $\Omega_{\text{FEM}}$ .
- 2: Compute  $\varepsilon_{hk}, \sigma_{hk}$  on mesh  $K_{hk}$  according to the CGA algorithm.
- 3: Refine locally such elements in the finite element mesh  $K_{hk}$  where

$$|h\varepsilon_{hk}| \geq \tilde{\beta}_{\varepsilon_k} \max_{K \in K_{hk}} |h\varepsilon_{hk}|,$$

$$|h\sigma_{hk}| \geq \tilde{\beta}_{\sigma_k} \max_{K \in K_{hk}} |h\sigma_{hk}|.$$

Here,  $\tilde{\beta}_{\varepsilon_k} \in (0, 1), \tilde{\beta}_{\sigma_k} \in (0, 1)$  are constants chosen by the user.

- 4: Construct the new mesh  $K_{hk+1}$  and interpolate  $\varepsilon_{hk}, \sigma_{hk}$  as well as measurements  $E_{\text{obs}}$  onto it.
  - 5: Terminate the algorithm if either  $\|\varepsilon_{hk+1} - \varepsilon_{hk}\| < \theta_{\varepsilon}^1$ , or  $\|\sigma_{hk+1} - \sigma_{hk}\| < \theta_{\sigma}^1$ , or  $\|g_{\varepsilon}^m\| < \theta_{\varepsilon}^2$ , or  $\|g_{\sigma}^m\| < \theta_{\sigma}^2$ , ( $m$  is the iteration in CGA), where  $\theta_{\varepsilon}^1, \theta_{\varepsilon}^2, \theta_{\sigma}^1$  and  $\theta_{\sigma}^2$  are tolerances chosen by the user. Otherwise, set  $k := k + 1$  and repeat the algorithm from step 2.
- 

C++ using the PETSc-based [36] WavES library [42]. Visualization of the three-dimensional results is performed using ParaView and GiD.

## 8.1 2D tests

The aim of this section is to present the results of applying our theory numerically in a 2D setting. This was done in two different tests. Before we get into the details, we specify the two-dimensional domain, which is considered to be  $\Omega = \{(x, y) : x \in (0, 1), y \in (0, 1)\}$  in space, and  $\Omega_T := \Omega \times (0, 1.2]$  in space and time. Our exact coefficients  $\varepsilon$  and  $\sigma$  that we aim to reconstruct are defined as

$$\begin{aligned} \varepsilon(x, y) &:= 1 + 3e^{-((x-0.5)^2 + (y-0.7)^2)/0.002}, \\ \sigma(x, y) &:= 1 + \frac{3}{2}e^{-((x-0.5)^2 + (y-0.7)^2)/0.002}. \end{aligned}$$

These constructions are somewhat realistic and inspired by studies [12], while also being in line with assumptions (2.9). Figure 1-c) and Figure 4-c) show spatial distribution of exact functions  $\varepsilon$  and  $\sigma$ , correspondingly. These coefficients were then reconstructed by choosing some initial guess for each,  $\varepsilon^0$  and  $\sigma^0$ , and then applying conjugate gradient Algorithm 1 of section 7.

In the two-dimensional numerical tests, we also use an approximation of system (2.8a–c), a damped wave system. Recently in [34] it was shown that in the computational setting using plane waves Maxwell's equations can be approximated by the acoustic wave equation. Since in our two-dimensional numerical simulations we are initializing a plane wave only for the one component of the electric field then accordingly to [34] the Maxwell' system can be approximated by the damped wave equation in the case of the conductive media. Before we introduce it, we define the boundaries

$\Gamma_i$ ,  $i = 1, 2, 3, 4$ , as the left, lower, right and upper sides of the unit square. Moreover, we let  $\Gamma_{i,T} := \Gamma_i \times [0, 1.2]$ , and specifically for the left side  $\Gamma_{1,t} = \Gamma_1 \times [0, \frac{\pi}{10}]$ . Now, we define the system used for numerical examples as

$$\begin{cases} \varepsilon \partial_{tt} E + \sigma \partial_t E - \Delta E = 0 & \text{for } (x, y, t) \in \Omega_T, & (8.1a) \\ E(x, y, 0) = 0, \partial_t E(x, y, 0) = 0 & \text{for } (x, y) \in \Omega, & (8.1b) \\ \partial_n E = \sin(20t) & \text{for } (x, y, t) \in \Gamma_{1,t}, \\ \partial_n E = -\partial_t E & \text{for } (x, y, t) \in \Gamma_3 \cup \Gamma_{1,T} \setminus \Gamma_{1,t}, & (8.1c) \\ \partial_n E = 0 & \text{for } (x, y, t) \in \Gamma_2 \cup \Gamma_4, \end{cases}$$

The system above represents introducing one period of a planar wave,  $\sin(20t)$ , from the boundary  $\Gamma_1$ , and after that make use of absorbing boundary conditions, while  $\Gamma_2$  and  $\Gamma_4$  are governed by homogeneous Neumann conditions.

Before getting into the results, we will define errors which we have studied computationally : relative  $L^2$  norms and supremum,  $\infty$  norms. This means that, for example, the relative  $L^2$  error for  $\varepsilon$  and  $\sigma$  are calculated as

$$e_\varepsilon^m := \frac{\|\varepsilon^m - \varepsilon\|}{\|\varepsilon\|}, \quad e_\sigma^m := \frac{\|\sigma^m - \sigma\|}{\|\sigma\|}, \quad (8.2)$$

where  $\varepsilon^m$  and  $\sigma^m$  are the reconstructed coefficients after  $m$  iterations of conjugate gradient Algorithm 1. The supremum errors are calculated in the same fashion but with the supremum norm instead of the  $L^2$  norm. The errors  $e_E^m$  for the discrepancy term  $E - \tilde{E}_{\text{obs}}$  were calculated as

$$e_E^m := \frac{\|E^m - \tilde{E}_{\text{obs}}\|}{\|E^m\|}, \quad (8.3)$$

where  $E^m := E(\varepsilon^m, \sigma^m)$ ,  $E := E(\varepsilon, \sigma)$  and  $\tilde{E}_{\text{obs}} = E + \delta$  where  $\delta \sim N(0, 0.1)$ . As for the coefficients, the supremum errors are calculated the same way, just with the supremum norm.

The following results come from two different tests, using two different sets of initial guesses in the settings described above.

**Test 1:** In the first test, we use the initial guesses  $\varepsilon^0(x, y) := 1$  and  $\sigma^0(x, y) := 1$ , representing the values of background medium. The reconstructions  $\varepsilon^{100}$  and  $\sigma^{100}$ , made after 100 conjugate gradient steps can be seen in Figure 1. One can immediately note that the reconstruction of  $\varepsilon$  is quite localized in the regions we expect, and while the  $\sigma$  reconstruction does not seem to be correctly localized in the  $x$ -direction, it does seem to be localized in the  $y$ -direction.

Analyzing the results further in Figure 2, we observe that the  $L^2$  errors and supremum errors decay consistently for both coefficients  $\varepsilon$ ,  $\sigma$ , as well as for  $E - \tilde{E}_{\text{obs}}$ . We note the exception of the supremum norm of  $E - \tilde{E}_{\text{obs}}$ , and a slight upwards trend at latter iterations in the  $L^2$  error of  $\sigma$ . However, these deviations could be the result of reaching a local minima, since we are using conjugate gradient method. These disturbances disappear as an initial guesses  $\varepsilon^0, \sigma^0$  becomes closer to the exact values of coefficients  $\varepsilon, \sigma$ . We will show this in the Test 2.

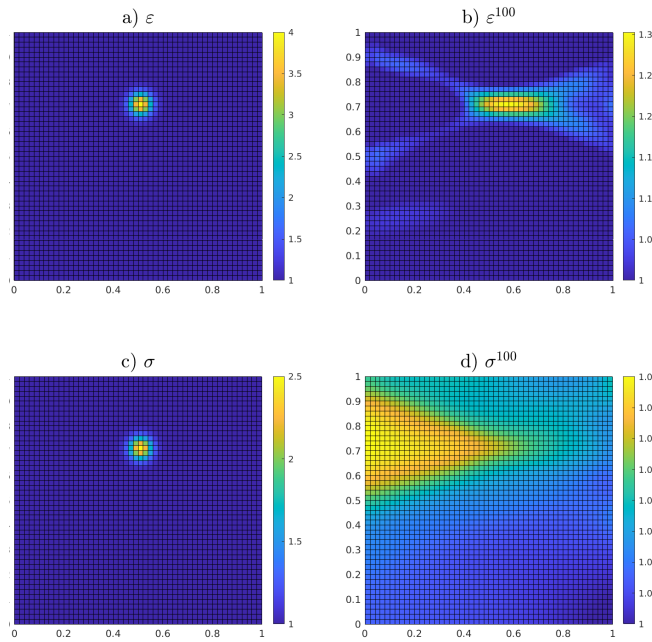


Figure 1: 2D tests, test 1. Results from CGA, Algorithm 1. Figures a) and b) are connected to  $\varepsilon$ : a) exact  $\varepsilon$ , b) reconstructed  $\varepsilon^{100}$  after 100 iterations in CGA. Figures c) and d) are connected to  $\sigma$ : c) exact  $\sigma$ , d) reconstructed  $\sigma^{100}$  after 100 iterations in CGA.

Finally, we can affirm the claims we made, by looking further at the norms of the adjoint problem solution  $\|\lambda\|$ , and norms of the gradients  $\|g_\varepsilon\|$  and  $\|g_\sigma\|$  shown in Figure 3. We observe that the norm of the adjoint problem solution and the gradients decay, which is to be expected from Theorem 4.2 as well as from the conjugate gradient Algorithm 1.

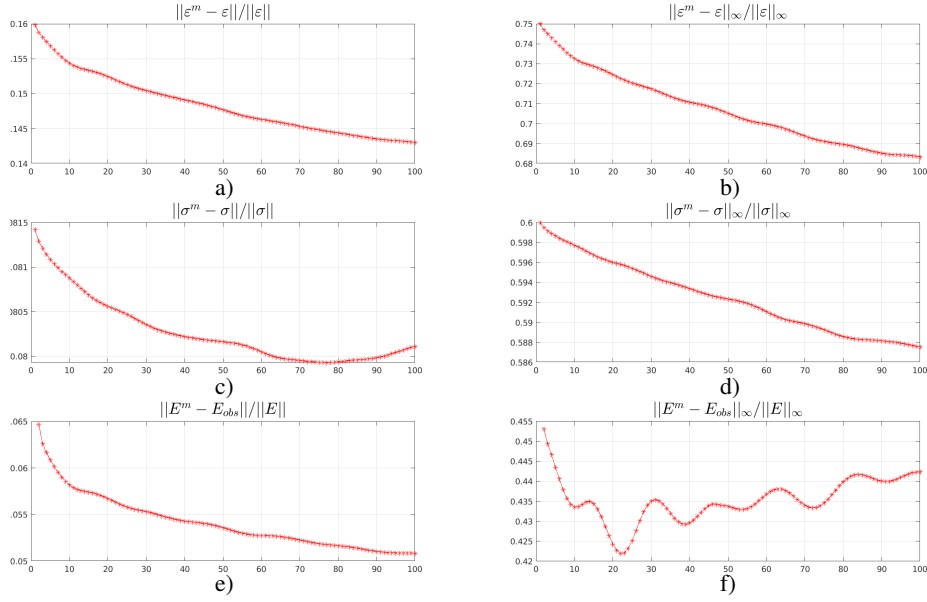


Figure 2: 2D tests, test 1. Convergence plots of errors over CGA iterations: a), b) errors  $e_\epsilon^m$  concerning  $\epsilon$ ; c), d) errors  $e_\sigma^m$  concerning  $\sigma$ ; e), f) errors  $e_E^m$  concerning the term  $E - \tilde{E}_{\text{obs}}$ . We note that figures a), c) and e) show the relative  $L^2$ -errors, and figures b), d) and f) show the supremum norms.

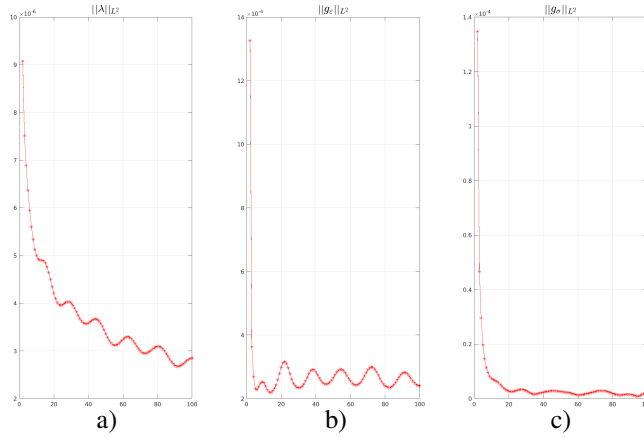


Figure 3: 2D tests, test 1. Convergence plots of  $L^2$  norms over CGA iterations: a)  $\|\lambda\|$ ; b)  $\|g_\epsilon\|$ ; c)  $\|g_\sigma\|$ .

**Test 2:** The second test was made the same way as the first, just with new initial guesses. These initial guesses were informed by the exact coefficients, but slightly perturbed, to see how the algorithms performed when initiated close to the global optima.

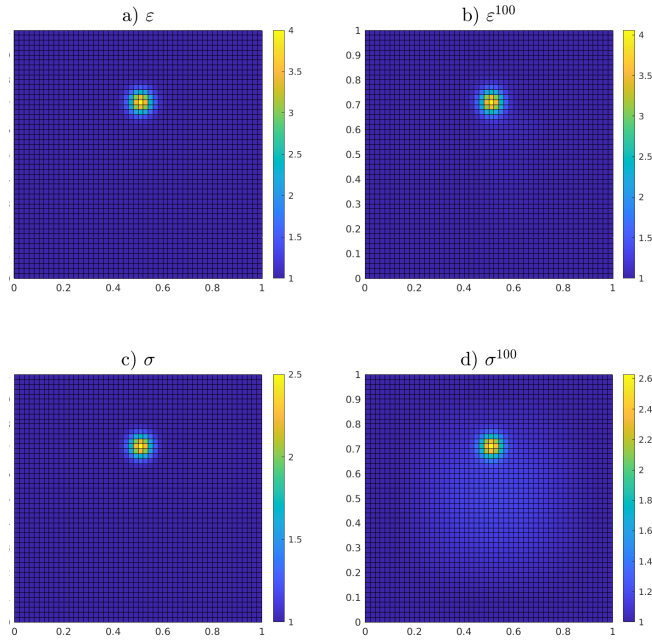


Figure 4: 2D tests, test 2. Results from CGA, Algorithm 1. Figures a) and b) are connected to  $\varepsilon$ : a) exact  $\varepsilon$ , b) reconstructed  $\varepsilon^{100}$  after 100 iterations in CGA. Figures c) and d) are connected to  $\sigma$ : c) exact  $\sigma$ , d) reconstructed  $\sigma^{100}$  after 100 iterations in CGA.

The initial guesses were defined as

$$\begin{aligned}\varepsilon^0(x, y) &:= \varepsilon(x, y) + 20\|\varepsilon\|_\infty x^2 y^2 (1-x)^2 (1-y)^2, \\ \sigma^0(x, y) &:= \sigma(x, y) + 20\|\sigma\|_\infty x^2 y^2 (1-x)^2 (1-y)^2,\end{aligned}$$

and the results of reconstruction can be seen in Figure 4. We observe that after initiating the Algorithm 1 close to the true values of the coefficients it does not deviate from the true solution. This conclusion is further strengthened in Figure 5, where we now observe how all errors decay consistently without exceptions as seen in the Test 1. This indicates that the conjugate gradient Algorithm 1 really converging towards the true value of parameters  $\varepsilon, \sigma$  and not to some local minimum.

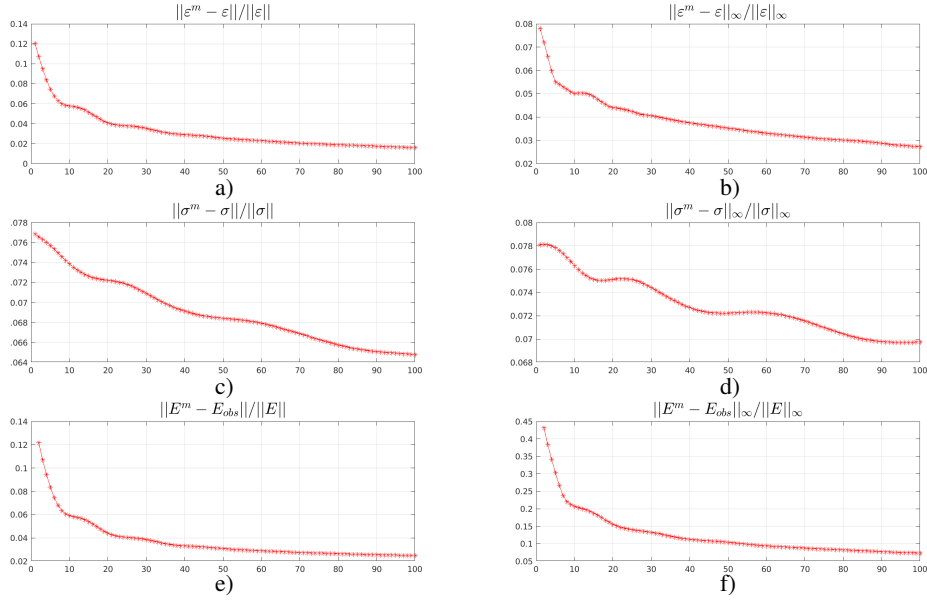


Figure 5: 2D tests, test 2. Convergence plots of errors over CGA iterations: a), b) errors  $e_\epsilon^m$  concerning  $\epsilon$ ; c), d) errors  $e_\sigma^m$  concerning  $\sigma$ ; e), f) errors  $e_E^m$  concerning the term  $E - \tilde{E}_{\text{obs}}$ . We note that figures a), c) and e) show the relative  $L^2$ -errors, and figures b), d) and f) show the supremum norms.

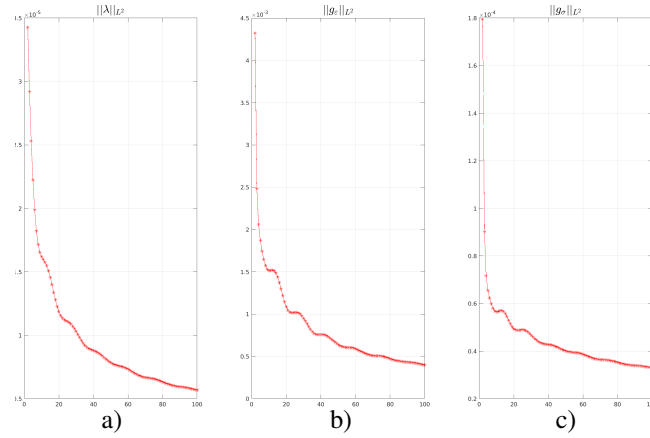


Figure 6: 2D tests, test 2. Convergence plots of  $L^2$  norms over CGA iterations: a)  $\|\lambda\|$ ; b)  $\|g_\epsilon\|$ ; c)  $\|g_\sigma\|$ .

Finally, in Figure 6 we see the same behavior as before, where the norms of  $\lambda$ ,  $g_\epsilon$  and  $g_\sigma$  tend towards zero or to stabilization what is in accordance with stopping criterion in the Algorithm 1.

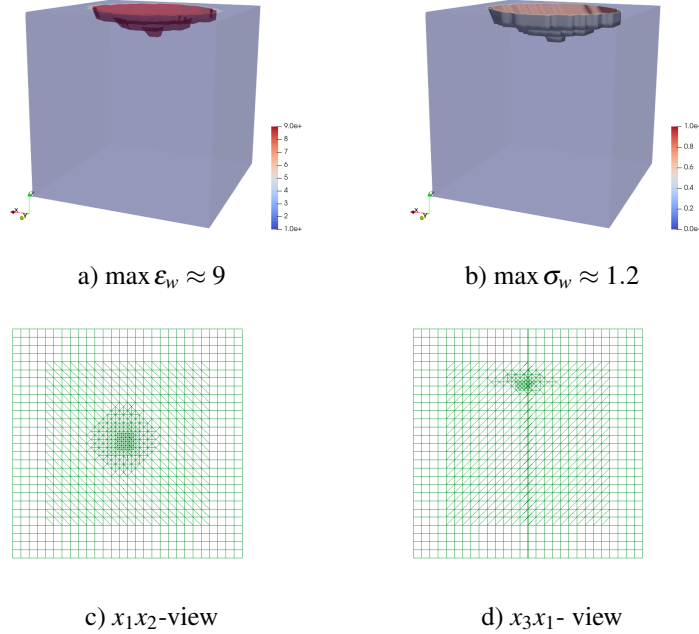


Figure 7: 3D tests, test 1. Dielectric weighted properties taken in our computations: a)  $\varepsilon_w$ , b)  $\sigma_w$ . c), d) Projections of the locally refined hybrid FE/FD mesh taken for generation of data.

## 8.2 3D tests

In this section we discuss three dimensional numerical results of reconstruction of both functions,  $\varepsilon$  and  $\sigma$ , in the model problem (8.4) using conjugate gradient algorithm (CGA) and adaptive conjugate gradient algorithm (ACGA) presented in section 7. ACGA is based on the local adaptive finite element mesh refinements utilizing a posteriori error indicators for the reconstruction of functions  $\varepsilon, \sigma$ . We refer to [5, 9, 11] for more details about this method.

For solutions of the forward and adjoint problems was used adaptive domain decomposition finite element/finite difference method (ADDFE/FDM) developed in [5, 8] and implemented in the software package WavES [42]. We refer to [5, 8] for details about numerical implementation of the ADDFE/FDM method for time-dependent Maxwell's system in conductive media.

In order to apply ADDFE/FDM in our computations we split the computational domain  $\Omega$  into two domains:  $\Omega_{\text{FEM}}$  where we apply the finite element method, and  $\Omega_{\text{FDM}}$  where we use the finite difference method, such that  $\Omega := \Omega_{\text{FEM}} \cup \Omega_{\text{FDM}}$  with  $\Omega_{\text{FEM}} \subset \Omega$ . We discretize the finite element domain  $\Omega_{\text{FEM}}$  by tetrahedral elements, and the finite difference domain  $\Omega_{\text{FDM}}$  - by hexahedral elements - see [5, 8] for further details of discretization in the ADDFE/FDM. In our computations we set the dimensionless compu-

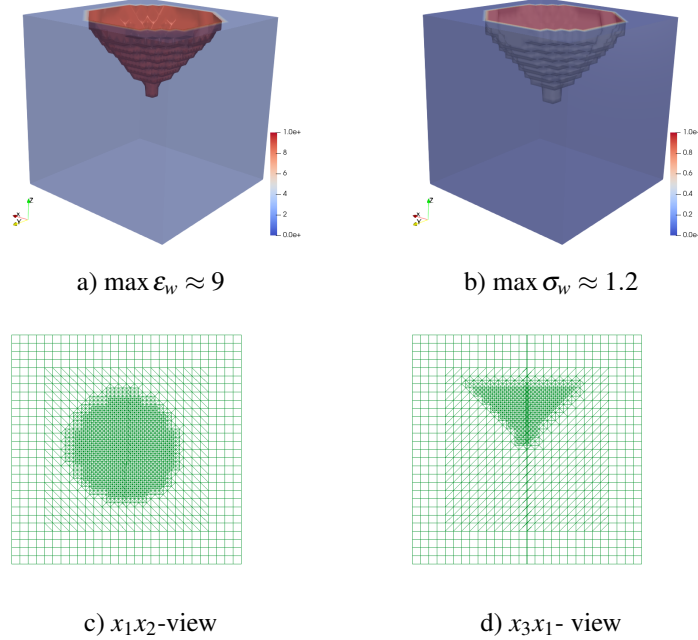


Figure 8: 3D tests, test 2. Dielectric weighted properties taken in our computations: a)  $\epsilon_w$ , b)  $\sigma_w$ . c), d) Projections of the locally refined hybrid FE/FD mesh taken for generation of data.

tational domain  $\Omega$  as  $\Omega = \{x = (x_1, x_2, x_3) \in (-2, 12) \times (-2, 12) \times (-2, 12)\}$ , and the computational domain  $\Omega_{\text{FEM}}$  as  $\Omega_{\text{FEM}} = \{x = (x_1, x_2, x_3) \in (0, 10) \times (0, 10) \times (0, 10)\}$ . The domain  $\Omega_{\text{FEM}}$  represents the 3D models of malign melanoma (MM) embedded within a homogeneous domain which has the size  $10 \times 10 \times 10$  mm. The geometrical models of MM growth were developed in [7] and they have realistic values of dielectric permittivity and conductivity of MM at 6 GHz. We note that based on geometrical models [7] in the recent work [10] were constructed the finite element meshes for MM growth on the skin, and two of them we use in the current tests. To proceed further, we assign values of  $\epsilon$  and  $\sigma$  in  $\Omega_{\text{FEM}}$  accordingly to the test values of the Table 1, and we set  $\epsilon = 1$  and  $\sigma = 0$  in  $\Omega \setminus \Omega_{\text{FEM}}$ . Figures 7, 8 show simplified models of MM placed in homogeneous domain with exact values of the relative dielectric permittivity and conductivity functions given in the Table 1. Dielectric properties shown on this figure have weighted values of  $\epsilon$  and  $\sigma$  which correspond to the test values presented in the Table 1. Our ongoing work is on the reconstructing non-weighted real values of  $\epsilon$  and  $\sigma$  presented in the Table 1, and will be reported later. To proceed further, we decompose the boundary  $\partial\Omega$  of the domain  $\Omega$  into three parts as follows:  $\partial\Omega = \partial_1\Omega \cup \partial_2\Omega \cup \partial_3\Omega$ . Here,  $\partial_1\Omega$  and  $\partial_2\Omega$  are, respectively, top and bottom sides of  $\Omega$ , and  $\partial_3\Omega$  is the union of left, right, front and back sides of this domain. The time-dependent observations are simulated at the backscattered boundary  $\Gamma_1 := \partial_1\Omega \times (0, T)$  of  $\Omega$ . We also define

$\Gamma_{1,1} := \partial_1 \Omega \times (0, t_1]$ ,  $\Gamma_{1,2} := \partial_1 \Omega \times (t_1, T)$ , and  $\Gamma_3 := \partial_3 \Omega \times (0, T)$ . In our computations we use the following stabilized model problem:

$$\begin{aligned} \varepsilon \partial_{tt} E + \nabla(\nabla \cdot E) - \Delta E - \nabla(\nabla \cdot (\varepsilon E)) &= -\sigma \partial_t E \text{ in } \Omega_T, \\ E(x, 0) = 0, \quad \partial_t E(x, 0) &= 0 \text{ in } \Omega, \\ \partial_n E &= P(t) \text{ on } \Gamma_{1,1}, \\ \partial_n E &= -\partial_t E \text{ on } \Gamma_{1,2} \cup \Gamma_2, \\ \partial_n E &= 0 \text{ on } \Gamma_3. \end{aligned} \tag{8.4}$$

We initialize a plane wave  $P(t) = (0, P_2, 0)(t)$  only for the one component  $E_2$  of the electric field  $E = (E_1, E_2, E_3)$  at  $\Gamma_{1,1}$  in (8.4) in time  $t = [0, 12.0]$  and define it as

$$P_2(t) = \begin{cases} \sin(\omega t), & \text{if } t \in (0, \frac{2\pi}{\omega}), \\ 0, & \text{if } t > \frac{2\pi}{\omega}. \end{cases} \tag{8.5}$$

Table 1: Tissue types and corresponding realistic values of  $\varepsilon$  and  $\sigma$  (S/m) at 6 Ghz for skin with malign melanoma (MM) used in our numerical experiments.

Tissue type	Real values		Test values		Depth (mm)
	$\varepsilon$	$\sigma$ (S/m)	$\varepsilon_w$	$\sigma_w$ (S/m)	
Immersion medium	32	4	1	0	2
Epidermis	35	4	1	0	1
Dermis	40	9	1	0	3.5
Fat	9	1	1	0	5.5
Tumor stage 1	45	6	8	1.2	< 1
Tumor stage 2	50	6	9	1.2	> 1
Tumor stage 3	60	6	-	-	> 1

Table 2: Geometrical properties of the MM models are taken from [7].

Month	Shape	Diameter (mm)	Depth (mm)
6	Cone	6.28	1.08
22	Cone	6.96	4.06

The goal of our numerical tests is to reconstruct weighted dielectric permittivity  $\varepsilon_w$  and conductivity  $\sigma_w$  functions for MM at month 6 and at month 22 with dielectric and geometrical properties presented in the Table 1 and in the Table 2, correspondingly, using time-dependent backscattered electric field  $E = (E_1, E_2, E_3)$  at  $\Gamma_1$ .

For generation of data we compute first components of the electric field  $E = (E_1, E_2, E_3)$  at  $\Gamma_1$  using known values of  $\varepsilon_w$  and  $\sigma_w$  given as the test values in the Table 1, and use them in the model problem (8.4). After we add the normally distributed Gaussian noise  $\delta = 10\%$  with the mean  $\mu = 0$  to the simulated electric field  $E = (E_1, E_2, E_3)$  at the

backscattered boundary  $\Gamma_1$ . Note that in order to avoid variational crimes the data is generated on the five time locally refined mesh which does not coincide with the finite element mesh used for computations in the ACGA. Figure 7 - c), d) and Figure 8 - c), d) show projections of locally refined finite element meshes used for generation of backscattered data in Test 1 and Test 2, correspondingly.

We have chosen numbers  $\tilde{\beta}_\varepsilon = 0.8, \tilde{\beta}_\sigma = 0.8$  in the mesh refinement criterion (7.5) in both tests. Relative errors presented in the Tables 3, 4 are computed as follows:

$$e_\varepsilon = \frac{\max_{\Omega_{\text{FEM}}} |\varepsilon_w - \varepsilon_{whk}|}{\text{nno} \cdot \max_{\Omega_{\text{FEM}}} |\varepsilon_w|}, \quad e_\sigma = \frac{\max_{\Omega_{\text{FEM}}} |\sigma_w - \sigma_{whk}|}{\text{nno} \cdot \max_{\Omega_{\text{FEM}}} |\sigma_w|}, \quad (8.6)$$

where nno is the number of nodes in the finite element mesh.

Table 3: *3D tests, test 1. Computational results of the reconstructions  $\varepsilon_{whk} := \max_{\Omega_{\text{FEM}}} \varepsilon_{whk}$ ,  $\sigma_{whk} := \max_{\Omega_{\text{FEM}}} \sigma_{whk}$  on a coarse and on adaptively refined meshes  $K_{hk}, k = 0, 1, 2, 3, 4$ , together with relative errors for obtained reconstructions. The noise level in the data for electric field is  $\delta = 10\%$ . Here,  $\max_{\Omega_{\text{FEM}}} \varepsilon_{whk}$ ,  $\max_{\Omega_{\text{FEM}}} \sigma_{whk}$  denote maximum of the computed functions  $\varepsilon_{wh}$ ,  $\sigma_{wh}$ , respectively, on  $k$  times refined mesh  $K_{hk}$ , in the domain  $\Omega_{\text{FEM}}$ , and  $M_k$  denotes the final number of iterations in the ACGA on  $k$  times refined mesh  $K_{hk}$  for reconstructed functions  $\varepsilon_{wh}$ ,  $\sigma_{wh}$ ,  $k = 0, 1, 2, 3, 4$ .*

Mesh	nno	$\ g_\varepsilon\ /\text{nno}$	$\ g_\sigma\ /\text{nno}$	$\varepsilon_{whk}$	$e_\varepsilon$	$\sigma_{whk}$	$e_\sigma$	$M_k$
$K_{h0}$	9261	7.8393e-06	9.2647e-06	6	3.5990e-05	0.25	8.5488e-05	2
$K_{h1}$	9261	7.7529e-06	1.1943e-05	9.5	6.0037e-06	0.6	5.3990e-05	1
$K_{h2}$	9261	7.7961e-06	1.1964e-05	10	1.1997e-05	0.64	5.0394e-05	1
$K_{h3}$	9261	7.8069e-06	1.0107e-05	10	1.1997e-05	0.95	2.2492e-05	1
$K_{h4}$	10116	6.9790e-06	6.3464e-06	10	1.0983e-05	1.0	1.6479e-05	1

Table 4: *3D tests, test 2. Computational results of the reconstructions  $\varepsilon_{whk} := \max_{\Omega_{\text{FEM}}} \varepsilon_{whk}$ ,  $\sigma_{whk} := \max_{\Omega_{\text{FEM}}} \sigma_{whk}$  on a coarse and on adaptively refined meshes  $K_{hk}, k = 0, 1, 2, 3, 4$ , together with relative errors for obtained reconstructions. The noise level in the data for electric field is  $\delta = 10\%$ . Here,  $\max_{\Omega_{\text{FEM}}} \varepsilon_{whk}$ ,  $\max_{\Omega_{\text{FEM}}} \sigma_{whk}$  denote maximum of the computed functions  $\varepsilon_{wh}$ ,  $\sigma_{wh}$ , respectively, on  $k$  times refined mesh  $K_{hk}$ , in the domain  $\Omega_{\text{FEM}}$ , and  $M_k$  denotes the final number of iterations in the ACGA on  $k$  times refined mesh  $K_{hk}$  for reconstructed functions  $\varepsilon_{wh}$ ,  $\sigma_{wh}$ ,  $k = 0, 1, 2, 3, 4$ .*

Mesh	nno	$\ g_\varepsilon\ /\text{nno}$	$\ g_\sigma\ /\text{nno}$	$\varepsilon_{whk}$	$e_\varepsilon$	$\sigma_{whk}$	$e_\sigma$	$M_k$
$K_{h0}$	9261	7.8393e-06	9.2647e-06	10	3.5990e-05	0.6	8.5488e-05	4
$K_{h1}$	11240	6.3879e-06	9.8399e-06	10	4.9466e-06	0.57	4.4484e-05	1
$K_{h2}$	18642	3.8730e-06	5.9436e-06	10	5.9597e-06	0.62	2.5035e-05	1
$K_{h3}$	50271	1.4382e-06	1.8619e-06	10	2.2100e-06	0.68	4.1435e-06	1
$K_{h4}$	177795	3.9709e-07	3.6109e-07	10	6.2488e-07	0.77	9.3760e-07	1

We take as an initial guess  $\varepsilon^0 = 1, \sigma^0 = 0$  for all points of the computational domain  $\Omega$  and run ACGA algorithm. This choice has shown good reconstruction results and has

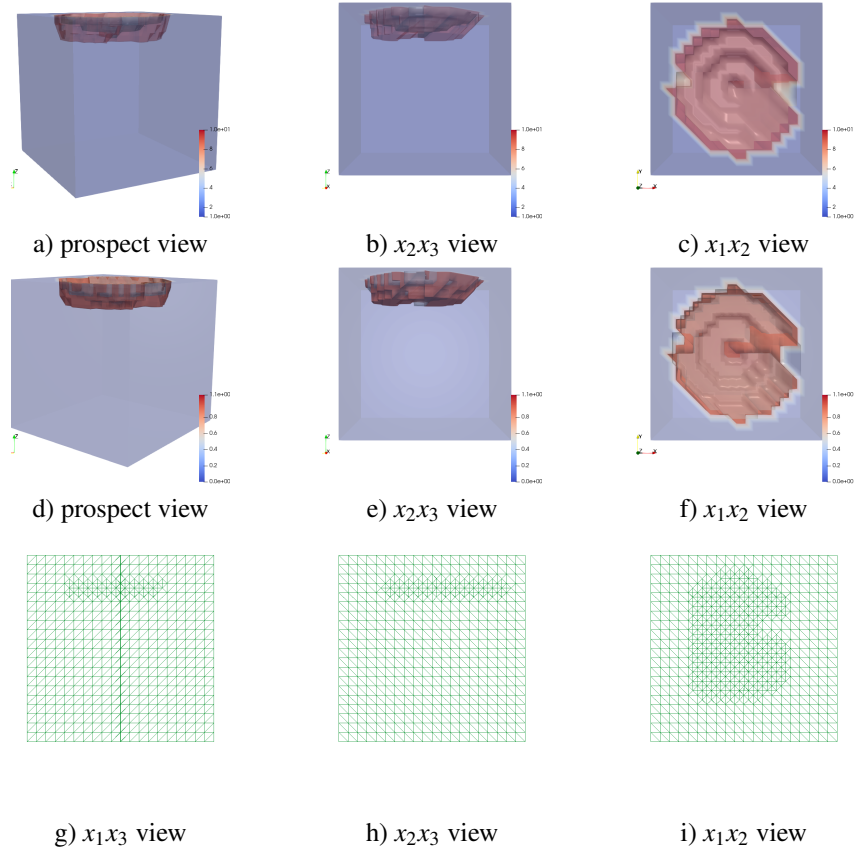


Figure 9: 3D tests, test 1. Performance of ACGA on the four times refined mesh  $K_{h4}$ . Isosurfaces of reconstruction for  $\max \varepsilon_{wh} \approx 9$  are presented in red color, and for  $\max \sigma_{wh} \approx 0.81$  are shown also in red color. a) - c) The weighted reconstruction of  $\varepsilon_{wh}$  (outlined in red color). d) - f) The weighted reconstruction of  $\sigma_{wh}$  (outlined in red color). g)-i) Projections of the adaptively refined mesh  $K_{h4}$ . The noise level in the data for electric field is  $\delta = 10\%$ . See Table 4 for obtained contrasts for  $\max_{\Omega_{\text{FEM}}} \varepsilon_{wh}$  and  $\max_{\Omega_{\text{FEM}}} \sigma_{wh}$  on meshes  $K_{hk}, k = 0, \dots, 4$ . For comparison we also present exact isosurfaces for  $\varepsilon_w$  and  $\sigma_w$  with values corresponding to the reconstructed ones, outlined in opaque.

been used in several previous computational studies - see details in [4, 5, 9, 11]. Physically it aligns with the initial computations taken in the homogeneous non-conductive domain.

### Test 1

Figures 9 show reconstruction of the weighted values of the relative dielectric permittivity and conductivity functions obtained by ACGA algorithm. Using this figure we observe that reconstructions of both functions converges to the depth of the MM as mesh refinements are applied. We also note that in this test the MM is located on the

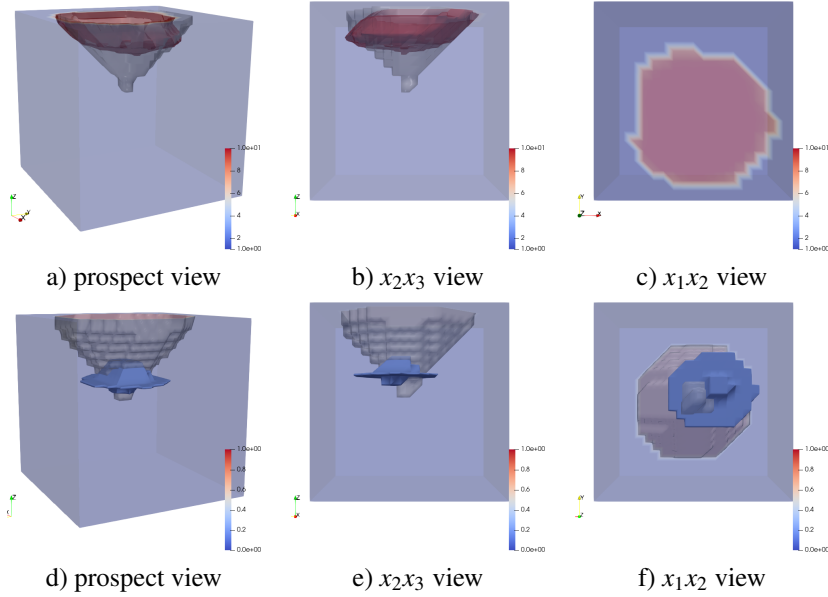


Figure 10: 3D tests, test 2. Performance of CGA on the coarse mesh  $K_{h0}$ . Isosurfaces of reconstruction for  $\max \epsilon_{wh} \approx 9$  are presented in red color, and for  $\max \sigma_{wh} \approx 0.6$  are shown in blue color. a) - c) The weighted reconstruction of  $\epsilon_{wh}$  (outlined in red color). d) - f) The weighted reconstruction of  $\sigma_{wh}$  (outlined in blue color). The noise level in the data for electric field is  $\delta = 10\%$ . See Table 4 for obtained contrasts for  $\max_{\Omega_{\text{FEM}}} \epsilon_{wh}$  and  $\max_{\Omega_{\text{FEM}}} \sigma_{wh}$ . For comparison we also present exact isosurfaces for  $\epsilon_w$  and  $\sigma_w$  with values corresponding to the reconstructed ones, outlined in opaque.

top of the backscattered domain and the depth of penetration inside the computational domain is only 1.08 mm. As a result, the maximal contrast for  $\epsilon_w$  is already achieved on the coarse mesh and further mesh refinements do not lead to a significant improvement in the contrast for  $\epsilon_w$ . However, the shape and the contrast for  $\sigma_w$  is improved significantly with mesh refinements. We refer to the Table 3 for obtained computational relative errors  $e_\epsilon, e_\sigma$  and contrasts for  $\max_{\Omega_{\text{FEM}}} \epsilon_{wh}$  and  $\max_{\Omega_{\text{FEM}}} \sigma_{wh}$ .

Since we selected numbers  $\tilde{\beta}_\epsilon = 0.8, \tilde{\beta}_\sigma = 0.8$  in the mesh refinement criterion in ACGA, the corresponding reconstructed values trigger mesh refinement only for  $k = 4$ . In other words, these parameters are too large for the Test 1, but we wanted to test the same parameters for both tests in order to ensure a more consistent and reliable comparison. We note that the same values  $\tilde{\beta}_\epsilon = 0.8, \tilde{\beta}_\sigma = 0.8$  provide very effective local mesh refinements for all meshes in Test 2.

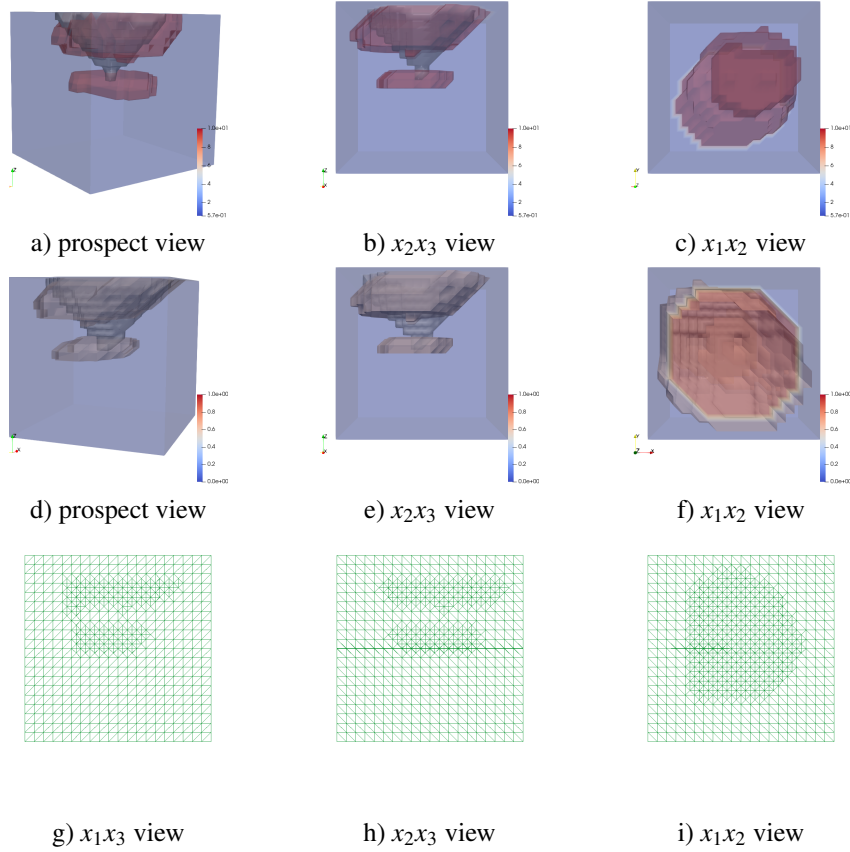


Figure 11: 3D tests, test 2. Performance of ACGA on the one time refined mesh  $K_{h1}$ . Isosurfaces of reconstruction for  $\max \varepsilon_{wh} \approx 9$  are presented in red color, and for  $\max \sigma_{wh} \approx 0.57$  are shown in rose color. a) - c) The weighted reconstruction of  $\varepsilon_{wh}$  (outlined in red color). d) - f) The weighted reconstruction of  $\sigma_{wh}$  (outlined in rose color). g)-i) Projections of the adaptively refined mesh  $K_{h1}$ . The noise level in the data for electric field is  $\delta = 10\%$ . See Table 4 for obtained contrasts for  $\max_{\Omega_{\text{FEM}}} \varepsilon_{wh}$  and  $\max_{\Omega_{\text{FEM}}} \sigma_{wh}$ . For comparison we also present exact isosurfaces for  $\varepsilon_w$  and  $\sigma_w$  with values corresponding to the reconstructed ones, outlined in opaque.

### Test 2

Figures 10, 11, and 12 show reconstruction of the weighted values of the relative dielectric permittivity and conductivity functions obtained by CGA and ACGA algorithms, respectively. Comparing results of the reconstruction shown on Figure 10 with reconstructions of Figure 11 and 12 we can conclude that the local adaptive mesh refinement, or ACGA algorithm, significantly improves results of 3D reconstruction of  $\varepsilon_w$  and  $\sigma_w$ . Using Figure 12 we observe that reconstructions of both functions converges to the depth of the MM as mesh refinements are applied. The final reconstructions are obtained on the 4 times locally refined mesh  $K_{h4}$  and are shown in the Figure 12.

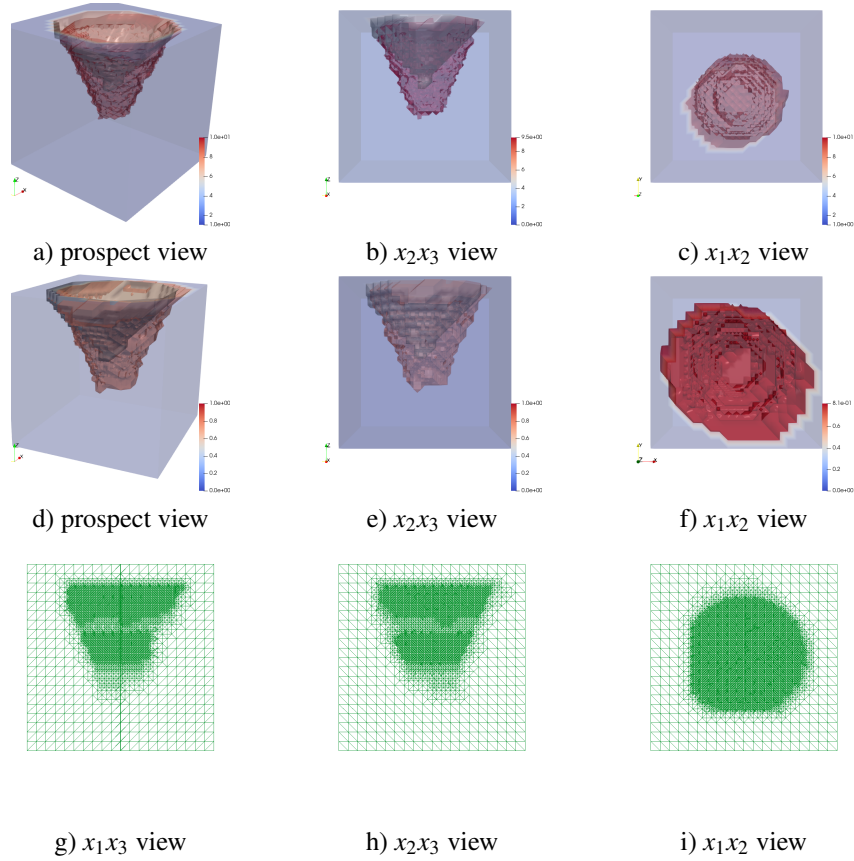


Figure 12: 3D tests, test 2. Performance of ACGA on the four times refined mesh  $K_{h4}$ . Isosurfaces of reconstruction for  $\max \varepsilon_{wh} \approx 9$  are presented in red color, and for  $\max \sigma_{wh} \approx 0.77$  are shown also in red color. a) - c) The weighted reconstruction of  $\varepsilon_{wh}$  (outlined in red color). d) - f) The weighted reconstruction of  $\sigma_{wh}$  (outlined in red color). g)-i) Projections of the adaptively refined mesh  $K_{h4}$ . The noise level in the data for electric field is  $\delta = 10\%$ . See Table 4 for obtained contrasts for  $\max_{\Omega_{\text{FEM}}} \varepsilon_{wh}$  and  $\max_{\Omega_{\text{FEM}}} \sigma_{wh}$ . For comparison we also present exact isosurfaces for  $\varepsilon_w$  and  $\sigma_w$  with values corresponding to the reconstructed ones, outlined in opaque.

From this figure, we also observe that the conical shape of the obtained reconstructions accurately represents the shape of the MM at a depth of 4.06 mm, consistent with the mesh refinements (see Figures 12-g, h, i) ) though the depth of the reconstructed MM is slightly overestimated. We refer to the Table 4 for obtained computational relative errors  $e_\varepsilon, e_\sigma$  and contrasts for  $\max_{\Omega_{\text{FEM}}} \varepsilon_{wh}$  and  $\max_{\Omega_{\text{FEM}}} \sigma_{wh}$  on locally adaptively refined meshes. We hope that performing the initial computations on a finer mesh with a size of  $h = 0.25$  instead of  $h = 0.5$  will provide a more accurate depth for the MM in Test 2. This hypothesis requires more computational resources and can be tested in future.

## 9 Conclusions

In the current work we developed variational optimization approach for reconstruction of dielectric permittivity and conductivity functions using time-dependent scattered measurements of the electric field collected at the part of the boundary of the computational domain. This is typical CIP which is an ill-posed problem. We solve CIP by minimizing the regularised Tikhonov's functional via Lagrangian approach. We present Lagrangian, derive optimality conditions and establish proofs for stability estimates for the forward and adjoint problems. Further, we present proof of the Fréchet differentiability of the regularized Tikhonov's functional and existence result of the solution of CIP. Our two- and three-dimensional computational tests show qualitative and quantitative reconstruction of dielectric permittivity and conductivity functions in several examples.

Future research will focus on reconstructing unweighted dielectric permittivity and conductivity functions for the detection of malignant melanoma on the skin, using both simulated and experimentally acquired data. This effort will require the development of a new adaptive DDFE/FDM method, specifically designed for finite difference domains, in which a damped wave equation replaces the acoustic model.

## Acknowledgment

The research of authors is supported by the Swedish Research Council grant VR 2024-04459 and STINT grant MG2023-9300.

## References

- [1] O. Abuzagheh, B. D. Barkana, and M. Faezipour, "Noninvasive real-time automated skin lesion analysis system for melanoma detection and prevention," *IEEE J. Trans. Eng. Health Med.*, vol. 3, 2015, Art. no. 4300212, doi: 10.1109/JTEHM.2015.2419612.
- [2] M. Ambrosanio, M. T. Bevacqua, J. LoVetri, V. Pascazio and T. Isernia, "In-Vivo Electrical Properties Estimation of Biological Tissues by Means of a Multi-Step Microwave Tomography Approach," in *IEEE Transactions on Medical Imaging*, vol. 43, no. 5, pp. 1983-1994, May 2024, doi: 10.1109/TMI.2024.3354463
- [3] F. Assous, P. Degond, E. Heintze and P. Raviart, On a finite-element method for solving the three-dimensional Maxwell equations, *Journal of Computational Physics*, **109** (1993), 222–237.
- [4] A. Bakushinsky, M. Y. Kokurin, A. Smirnova: *Iterative Methods for Ill-posed Problems*, Inverse and Ill-Posed Problems Series 54, De Gruyter, 2011.
- [5] L. Beilina, E. Lindström: An Adaptive Finite Element/Finite Difference Domain Decomposition Method for Applications in Microwave Imaging. *Electronics* 2022, 11, 1359 2022.

- [6] L. Beilina, A. Eriksson and N. Neittaanmäki, Frequency inversion method and device for malignant melanoma detection using RF/microwaves, 2024 International Conference on Electromagnetics in Advanced Applications (ICEAA), Lisbon, Portugal, 2024, pp. 794-799, doi: 10.1109/ICEAA61917.2024.10701729.
- [7] J. Boparai, R. Tchinnov, O. Miller, Y. Jallouli and M. Popović, "Models of Melanoma Growth for Assessment of Microwave-Based Diagnostic Tools," in *IEEE Journal of Electromagnetics, RF and Microwaves in Medicine and Biology*, vol. 8, no. 3, pp. 305-315, Sept. 2024, doi: 10.1109/JERM.2024.3430315.
- [8] E. Lindström, L. Beilina: Energy norm error estimates and convergence analysis for a stabilized Maxwell's equations in conductive media. *Appl Math* 69, 415–436, 2024.
- [9] E. Lindström, L. Beilina, A hybrid finite element/finite difference method for reconstruction of dielectric properties of conductive objects, 2024 International Conference on Electromagnetics in Advanced Applications (ICEAA), Lisbon, Portugal, 2024, pp. 788-793, doi: 10.1109/ICEAA61917.2024.10701914
- [10] E. Lindström, L. Beilina, Finite element 3D models of melanoma growth and time-dependent backscattered data for dielectric properties of melanoma at 6 GHz, 2025 International Conference on Electromagnetics in Advanced Applications (ICEAA),Palermo, Italy, 2025. arXiv:2508.07794
- [11] L. Beilina, M.V. Klibanov: *Approximate global convergence and adaptivity for coefficient inverse problems*, Springer, New-York, 2012.
- [12] L., Beilina, V. Ruas: On the Maxwell-wave equation coupling problem and its explicit finite-element solution. *Appl Math* 68, 75–98 2023.
- [13] L. Beilina, N. T. Th'anh, M.V. Klibanov and J. B. Malmberg, Globally convergent and adaptive finite element methods in imaging of buried objects from experimental backscattering radar measurements, *Journal of Computational and Applied Mathematics, Elsevier*, DOI: 10.1016/j.cam.2014.11.055, 2015.
- [14] S. C. Brenner and L. R. Scott: *The Mathematical Theory of Finite Element Methods* (2nd edn), Springer-Verlag, New York, 2002.
- [15] P. Ciarlet, Jr., H. Wu and J. Zou: Edge element methods for Maxwell's equations with strong convergence for Gauss' laws, *SIAM Journal on Numerical Analysis* 52 (2014), 779-807.
- [16] R. Courant, K. Friedrichs and H. Lewy: On the partial differential equations of mathematical physics, *IBM Journal of Research and Development*, 11 (1967), 215-234.

- [17] *G. C. Cohen: Higher order numerical methods for transient wave equations*, Springer-Verlag, 2002.
- [18] *A. Elmkies and P. Joly: Finite elements and mass lumping for Maxwell's equations: the 2D case*, *Numerical Analysis*, **324** (1997), 1287–1293.
- [19] *H. W. Engl, M. Hanke and A. Neubauer: Regularization of Inverse Problems*, Boston, Kluwer Academic Publishers, 2000.
- [20] Fink C, Haenssle HA. Non-invasive tools for the diagnosis of cutaneous melanoma. *Skin Res Technol*. 2017 Aug;23(3):261-271. doi: 10.1111/srt.12350. Epub 2016 Nov 22. PMID: 27878858.
- [21] *B. Engquist and A. Majda: Absorbing boundary conditions for the numerical simulation of waves*, *Mathematics of Computation*, **31** (1977), 629-651.
- [22] *K. Eriksson, D. Estep and C. Johnson: Calculus in Several Dimensions*, Springer, Berlin, 2004.
- [23] A. V. Goncharsky, S. Y. Romanov, A method of solving the coefficient inverse problems of wave tomography, *Comput. Math. Appl.*, 2019;77:967–980.
- [24] A. V. Goncharsky, S. Y. Romanov, S. Y. Seryozhnikov, Low-frequency ultrasonic tomography: mathematical methods and experimental results. *Moscow University Phys Bullet*. 2019;74(1): 43–51.
- [25] Editor(s): Pierre Grangeat, *Tomography*, Wiley, 2009, DOI:10.1002/9780470611784
- [26] *K Ito, B Jin, and T Takeuchi: Multi-parameter Tikhonov regularization*, *Methods and Applications of Analysis*, **18** (2011), 31–46.
- [27] W.T. Joines, Y. Zhang, C. Li, and R. L. Jirtle, The measured electrical properties of normal and malignant human tissues from 50 to 900 MHz', *Med. Phys.*, 21 (4), pp.547-550, 1994.
- [28] *C. Johnson: Numerical Solution of Partial Differential Equations by the Finite Element Method*, Dover Books on Mathematics, 2009.
- [29] Vo Anh Khoa, Grant W. Bidney, Michael V. Klibanov, Loc H. Nguyen, Lam H. Nguyen, Anders J. Sullivan & Vasily N. Astratov (2021), An inverse problem of a simultaneous reconstruction of the dielectric constant and conductivity from experimental backscattering data, *Inverse Problems in Science and Engineering*, 29:5, 712-735, DOI: 10.1080/17415977.2020.1802447
- [30] *M. Křížek, P. Neittaanmäki: Finite element approximation of variational problems and applications*, Longman, Harlow, 1990.
- [31] *O. A. Ladyzhenskaya: Boundary Value Problems of Mathematical Physics*, Springer Verlag, Berlin, 1985.

- [32] C. D. Munz, P. Omnes, R. Schneider, E. Sonnendrucker and U. Voss: Divergence correction techniques for Maxwell Solvers based on a hyperbolic model, *Journal of Computational Physics*, **161** (2000), 484–511.
- [33] O. Pironneau: *Optimal shape design for elliptic systems*, Springer-Verlag, Berlin, 1984.
- [34] Romanov, Vladimir G. and Klibanov, Michael V. "Can a single scalar second order PDE govern well the propagation of the electric wave field in a heterogeneous 3D medium?" *Journal of Inverse and Ill-posed Problems*, vol. 30, no. 4, 2022, pp. 595-611. <https://doi.org/10.1515/jiip-2021-0085>
- [35] D. R. Smith, S. Schultz, P. Markos and C. M. Soukoulis: Determination of effective permittivity and permeability of metamaterials from reflection and transmission coefficients, *Physical Review B*, **65** (2002), DOI:10.1103/PhysRevB.65.195104.
- [36] *PETSc, Portable, Extensible Toolkit for Scientific Computation*, <http://www.mcs.anl.gov/petsc/>.
- [37] N. T. Thánh, L. Beilina, M. V. Klibanov, and M. A. Fiddy, Reconstruction of the refractive index from experimental backscattering data using a globally convergent inverse method, *SIAM J. Sci. Comput.*, 36 (2014), pp. B273-B293.
- [38] N. T. Thánh, L. Beilina, M. V. Klibanov, M. A. Fiddy, Imaging of Buried Objects from Experimental Backscattering Time-Dependent Measurements using a Globally Convergent Inverse Algorithm, *SIAM Journal on Imaging Sciences*, 8(1), 757-786, 2015.
- [39] A.N. Tikhonov, A.V. Goncharsky, V.V. Stepanov and A.G. Yagola: *Numerical Methods for the Solution of Ill-Posed Problems*, London: Kluwer, London, 1995.
- [40] Tikhonov A.N., Goncharskiy A.V., Stepanov V.V., Kochikov I.V.: Ill-posed problems of the image processing, *DAN USSR*, 294 (4), 832-837, 1987.
- [41] M. Pastorino, *Microwave Imaging*, John Wiley & Sons, Hoboken, NJ, 2010.
- [42] *WavES: the software package*, <http://www.waves24.com>
- [43] E. Zeidler, *Applied Functional Analysis: Main Principles and Their Applications*, Springer, 1995.